

RESEARCH

Open Access



Conventional, functional and radiomics assessment for intrahepatic cholangiocarcinoma

Vincenza Granata^{1*}, Roberta Fusco², Andrea Belli³, Valentina Borzillo⁴, Pierpaolo Palumbo^{5,6}, Federico Bruno^{6,7}, Roberta Grassi⁸, Alessandro Ottaiano⁹, Guglielmo Nasti⁹, Vincenzo Pilone¹⁰, Antonella Petrillo¹ and Francesco Izzo³

Abstract

Background: This paper offers an assessment of diagnostic tools in the evaluation of Intrahepatic Cholangiocarcinoma (ICC).

Methods: Several electronic datasets were analysed to search papers on morphological and functional evaluation in ICC patients. Papers published in English language has been scheduled from January 2010 to December 2021.

Results: We found that 88 clinical studies satisfied our research criteria. Several functional parameters and morphological elements allow a truthful ICC diagnosis. The contrast medium evaluation, during the different phases of contrast studies, support the recognition of several distinctive features of ICC. The imaging tool to employed and the type of contrast medium in magnetic resonance imaging, extracellular or hepatobiliary, should change considering patient, departement, and regional features. Also, Radiomics is an emerging area in the evaluation of ICCs.

Post treatment studies are required to evaluate the efficacy and the safety of therapies so as the patient surveillance.

Conclusions: Several morphological and functional data obtained during Imaging studies allow a truthful ICC diagnosis.

Keywords: ICC, Ultrasound, Computed tomography, Magnetic resonance imaging, Radiomics

Introduction

Primary liver cancer, including hepatocellular carcinoma (HCC), intrahepatic cholangiocarcinoma (ICC) and other rare types, is the sixth most usually detected tumour and the third leading cause of tumour death worldwide [1–3].

In line with the Liver Cancer Study Group of Japan, based on the macroscopic growth pattern, ICC can be categorised as mass forming, periductal infiltrating, or intraductal growing type [4–9]. The mass forming is the

most frequent, accounting for 78% of all cases of ICC [10–12]. Periductal infiltrating tumours develop alongside the bile ducts, producing bile duct wall thickening, luminal stenosis and proximal biliary dilatation [7–9]. This type represents about 16% of all ICCs, but it is the most common at hilar side [12]. Intraductal growing CC is the rarest form [12].

ICC could have an abundant stromal fibrosis, features that is infrequent in perihilar type, but usually found in peripheral type [12]. This datum is revealed into imaging. An appropriate diagnosis is crucial since radical surgery is the only curative treatment [10]. Multiphasic contrast-enhanced computed tomography (CT) and magnetic resonance imaging (MRI) are imaging tools to choosing in ICC patients. In the pre-surgical assessment phase, a multimodal strategy should be favorite in order to use the

*Correspondence: v.granata@istitutotumori.na.it

¹ Division of Radiology, "Istituto Nazionale Tumori IRCCS Fondazione Pascale – IRCCS di Napoli", 80131 Naples, Italy
Full list of author information is available at the end of the article



© The Author(s) 2022, corrected publication 2022. **Open Access** This article is licensed under a Creative Commons Attribution 4.0 International License, which permits use, sharing, adaptation, distribution and reproduction in any medium or format, as long as you give appropriate credit to the original author(s) and the source, provide a link to the Creative Commons licence, and indicate if changes were made. The images or other third party material in this article are included in the article's Creative Commons licence, unless indicated otherwise in a credit line to the material. If material is not included in the article's Creative Commons licence and your intended use is not permitted by statutory regulation or exceeds the permitted use, you will need to obtain permission directly from the copyright holder. To view a copy of this licence, visit <http://creativecommons.org/licenses/by/4.0/>. The Creative Commons Public Domain Dedication waiver (<http://creativecommons.org/publicdomain/zero/1.0/>) applies to the data made available in this article, unless otherwise stated in a credit line to the data.

pros and cons of CT and MRI. In fact, the high spatial resolution provided by CT with the high soft tissue contrast by MRI favours a more accurate assessment. Additionally, thanks to the ability of correlate morphological and functional features, MRI allows a suitable characterization of liver lesion. Also, the different contrast agent for MRI could influence diagnosis considering the differences between hepatobiliary agents (HBAs) and extracellular agents (ECAs) [13–21]. Also, Diffusion Weighted Imaging (DWI) has been employed to assess focal liver lesions (FLL). [14].

When the patient is unfit for surgical resection, locoregional therapies should be considered in order to delay disease progression and prolong life or as a bridge to curative treatment (i.e. downstaging). For ICCA, trans-arterial chemoembolization (TACE), drug-eluting bead trans-arterial chemoembolization (DEB-TACE), radiofrequency ablation (RFA), microwave ablation (MWA), trans-arterial-radioembolization (Yttrium90; TARE), and reversible electroporation have been assessed [21–26]. Several researches have shown that these treatments, alone or in combination with chemotherapy, improve Overall Survival (OS) [24]. In a cohort of non surgical treated small (≤ 5 cm) iCCA, staged as AJCC I/II, RFA-treated patients showed better survival respect to chemoradiotherapy [23], results reported by a recent meta-analysis, too [24]. Consequently, RFA is the treatment of choice in small ICCs. In this scenario, assessment post treatment is a new challenge for radiologists [25–29].

In this narrative review we reported an overview and update on ICC assessment in staging and post treatment phase.

Methods

This study is autonomous without protocol and registration number.

We analysed several electronic datasets: PubMed (US National Library of Medicine, <http://www.ncbi.nlm.nih.gov/pubmed>), Scopus (Elsevier, <http://www.scopus.com/>), Web of Science (Thomson Reuters, "<http://apps.webofknowledge.com>) and Google Scholar (<https://scholar.google.it/>), using the subsequent keywords: “ICC” AND “Ultrasound”, “ICC” AND “Computed Tomography”, “ICC” AND “Magnetic Resonance Imaging”, “ICC” AND “Radiomics”, “ICC” AND “Li-RADS”, “ICC” AND “Ablative Therapies” AND “Assessment”.

Papers published in English language has been scheduled from January 2010 to December 2021. All titles and abstract were assessed, and full text was retrieved for each included article. Clinical studies (eg. retrospective analysis, case series, prospective cohort study) on morphological and functional diagnostic assessment in staging and post treatment phase on ICC were retrieved. Exclusion criteria were inaccessibility of full text, case report, review, or letter to editors.

Results

We recognised 2201 pertinent papers. After deleting 1588 duplicates, we acquired 613 papers. We recognised 28 papers throughout visualizing reference lists of the aquired papers that we added to the 633 papers selected (total number of scrutinized articles was 641). Then we rejected 553 inappropriate papers throughout reading abstracts.

A total of 88 clinical studies were assessed in these narrative review. The reference flow is summarized in the study flow diagram (Fig. 1).

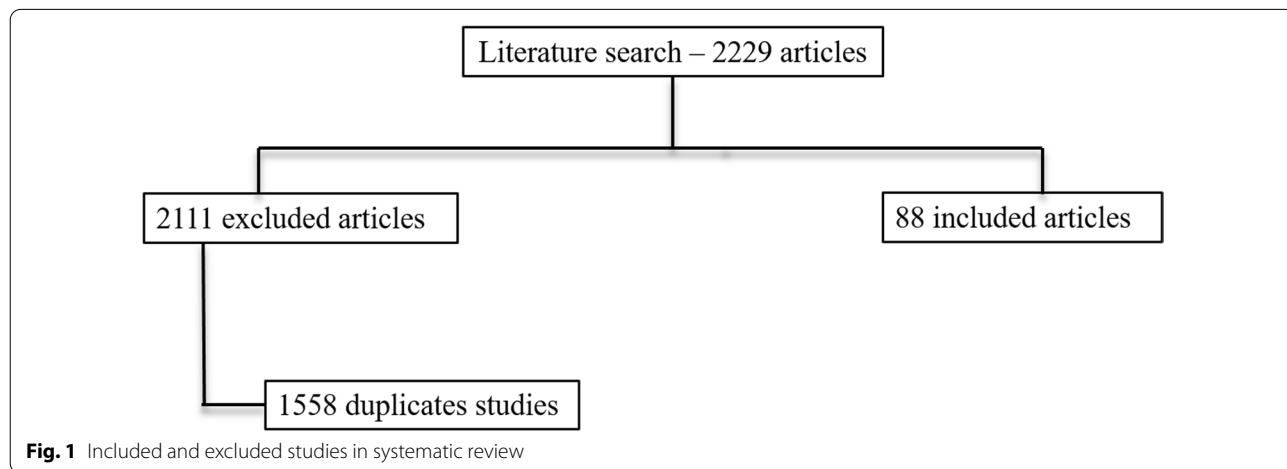


Fig. 1 Included and excluded studies in systematic review

Discussion

Diagnostic tools

Ultrasound

Ultrasound (US) is an imaging tool inexpensive, non-aggressive, non based on X-rays sources and so repeatable [30–40]. The possibility of injecting a contrast medium (Contrast-Enhanced Ultrasound (CEUS)) determines a technical evolution [30]. CEUS has a wide range of applications, being able to emphasize the large vessel flows and the microcirculation; therefore it has as its particular target the oncological setting [30–40]. The liver contrast study during CEUS includes: (1) arterial phase, which starts 10–20 s and ends 30–45 s after contrast injection; (b) portal venous phase, which lasts from 30–45 s to 2 min after contrast agent injection; and (c) the late phase, which lasts from 4 to 6 min after the contrast injection. It is possible to assess a post-vascular phase if used Sonazoid; during this phase is possible to assess the uptake of the contrast medium by Kupffer cells, in order to obtain functional parameters.

US with CEUS allows the first assessment of FLLs, helping in the differentiation between benign lesions (as haemangiomas) and malignant tumours.

Mass-forming ICC, on US studies, occurs as a large non-encapsulated mass with lobulated or variable shape. As associated features, it is possible see hepatic capsular

retraction and dilated peripheral bile ducts (Fig. 2), so as satellite lesions, near the primary lesion, and liver metastases. Necrosis, fibrosis and active growth tumour can cause lesion heterogeneous echogenicity [40]. During contrast study, ICC could show hyperenhancement during arterial phase (Fig. 3), with washout in late phase [40]. There is little agreement regarding the differential diagnosis between ICC and HCCC, on CEUS. ICC exhibits lesser enhancement in arterial phase with early (<60 s) and prominent washout compared to HCC [40–54]. Chen et al. demonstrated that the pooled sensitivity of CEUS in differentiating ICC from HCC was 0.92 and the pooled specificity was 0.87 [42].

The advantage of US/CEUS is the wide diffusion, the possibility to guide ablative procedures and to assess immediately the necrosis. In this scenario, the radiologist should be confident with this tool.

Computed tomography

Computed tomography is habitually the first diagnostic toll in the assessment of FLLs [55–63]. The post contrast enhancement patterns of FLLs are critical for categorizing lesions, and the CT image analysis, during characterization phase, allows the diagnosis of FLLs [55]. Yet, in modern clinical setting, this analysis could be prejudicate by the radiologist's skill [61, 64–69].

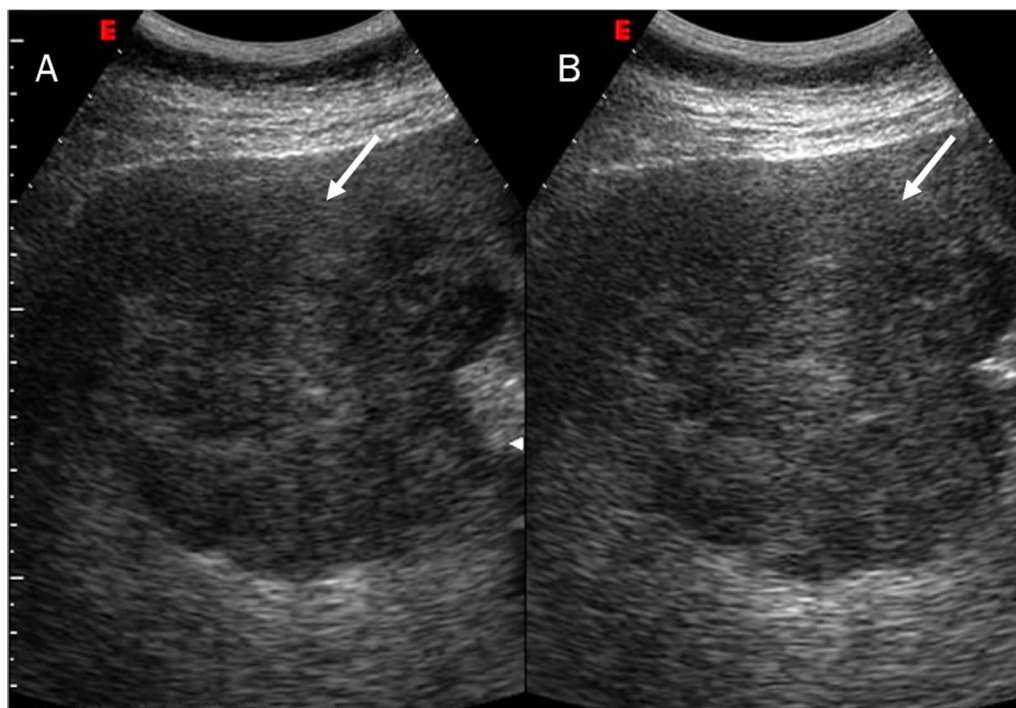


Fig. 2 US assessment of ICC on VIII-VII hepatic segment. The lesion (arrow) is sizeable mass of lobulated contour with heterogeneous echogenicity due to the interleaving of necrosis, fibrosis and active growth tissue

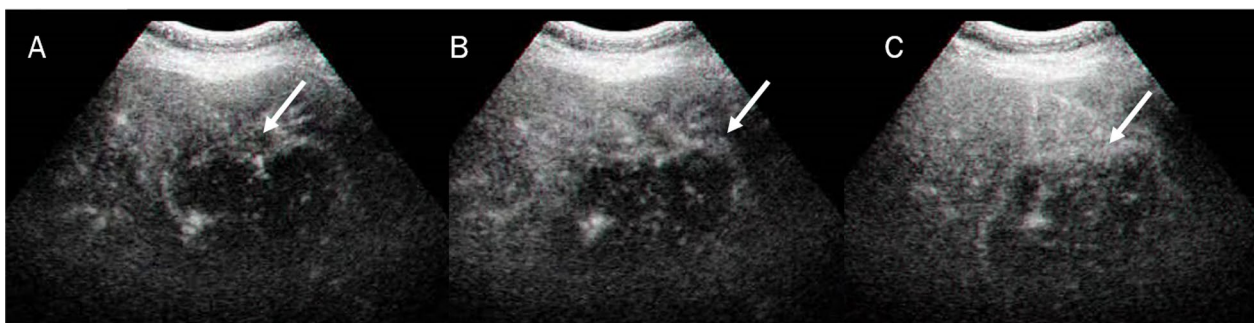


Fig. 3 CEUS assessment of ICC on V hepatic segment. The lesion shows peripheral rim hyperenhancement in arterial phase (A) and early (B) and marked (C) washout

CT is frequently the first diagnostic imaging technique to characterize ICC and contrarily to US/CEUS evaluation it is operator independent [70–79]. Although, Chen et al. [71] compared the enhancement pattern of ICC on CEUS with that on CT in 40 pathologically proven ICC lesions. The enhancement level and pattern in the post contrast phases on both CEUS and CT were assessed. CEUS made a correct diagnosis in 32 lesions while CT in 27 lesions. So, they demonstrated that CEUS had the same accuracy as CT in ICC diagnosing [71]. However, CT not only offers a complete evaluation of tumour, but also the association between the lesion and neighbouring structures as the hepatic artery, portal vein and biliary tree, so as the whole body surveillance for metastases assessment [53]. According to a recent meta-analysis, CT provides a satisfactory pooled sensitivity of 89% and pooled specificity of 92% for portal vein involvement and 84% pooled sensitivity and 93% pooled specificity for hepatic artery involvement in perihilar CC [77].

Typical study protocol includes several phases with and without contrast injection: non-contrast phase, arterial,

portal or venous, and delayed phase, which is obtained from 3–5 min to 30 min after contrast medium injection [53]. The non contrast phase allows the detection of intraductal stones. Arterial phase, performed 20–30 s after contrast medium injection, allows to assess arterial anatomy and to plan the surgical approach. Venous phase is performed 25–30 s after the completion of late arterial phase scanning. The usual CT pattern of a mass-forming ICC is a hypo-attenuated mass with irregular peripheral enhancement in the hepatic arterial phase, and gradual centripetal enhancement during venous and delayed phases (Fig. 4) [53]. This enhancement pattern is due to the histologically characteristic of the lesion, with the peripheral tissue which comprises viable cells, whereas the central portion comprises coagulative necrosis and fibrous stroma [53].

Latest techniques have been established to rise tumour detection, such as dual-energy CT (DECT) [80–92]. DECT, which is founded on instantaneously acquisition of two image datasets at different energy levels, can produce virtual monochromatic images

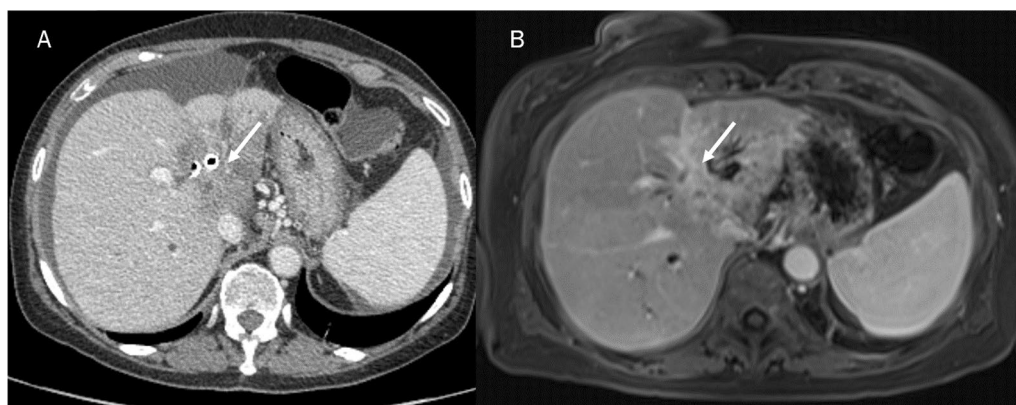


Fig. 4 CT (A) and MRI (B) portal phase assessment of ICC. The typical contrast enhancement is a gradual centripetal enhancement on dynamic studies (arrows)

(VMIs) [80]. Several researches demonstrated that DECT allowed considerably better focal liver lesion detection compared to conventional CT [93]. Additionally, radiation and contrast media dose decrease would mainly be beneficial for patient surveillance. Infact, radiation exposure is often underestimated in oncologic patients due to their relatively short life expectancy and the clinicians' focus on the immense benefit of early detection of recurrence [60–63].

Several researches assessed the role of DECT in the characterization of ICCs, with regard to the use of DECT quantitative parameters compared with the use of conventional CT for differentiating small (≤ 3 cm) intrahepatic mass-forming cholangiocarcinoma (IMCC) from small liver abscess (LA) during the portal venous phase (PVP) which showed greater accuracy than quantitative and qualitative analyses of conventional CT in these lesions [94, 95].

Perfusion CT (pCT) is a diagnostic method founded on contrast kinetics of tissue that provides quantitative data. pCT assesses dynamic variations in tissue iodine concentration over time, allowing to obtain tissue-specific data, including blood flow (BF), blood volume (BV), time to peak concentration (TTP), vascular permeability surface area product (PS), and permeability (K_{trans}), which can be utilised as biomarkers for tumour vascularization and perfusion. Several authors showed that pCT is a considerable tool for lesion characterization, treatment response assessment, and prognosis [96–101].

Zhao et al. [98] evaluated different perfusion parameters and corresponding histogram parameters compared to conventional post contrast CT analysis in differentiating ICC from HCC. They demonstrated that the mean value, and all the percentiles of the arterial enhancement fraction (AEF) were significantly higher in HCC than in ICC. The variance in hepatic arterial blood supply perfusion (HAP) and AEF for the mean perfusion data and all percentile parameters between lesion and normal liver were drastically higher in HCC than in ICC. The relative AEF was statistically significant between HCC and ICC. Among all parameters, the mean value of ΔAEF , the 75th percentiles of ΔAEF and $rAEF$, and the 25th percentile of HF_{tumor} had the highest sensitivities of 94.4%, while the 50th percentile of $rAEF$ had the highest specificity of 82.4%. AEF (including ΔAEF and $rAEF$) and the corresponding histogram parameters derived from triphasic CT aided accurate lesion diagnosis [98].

The CT is the most widely used tool in the assessment of FLLs, and the possibility to utilised new techniques, as DECT or perfusion, allow to choose the more appropriate study protocol considering patients and conventional features of lesions.

Magnetic resonance imaging

MRI is the more suitable tool in the assessment of FLL, thanks to its possibility to analyse functional and morphological data [102–115].

Morphological assessment

Several morphological patterns allow to identify ICCs. Granata et al. assessed MR features of 88 ICCs (61 mass-forming type; 23 periductal infiltrating tumours type and 4 intraductal growing type), showing that on T1-W sequences, among the 61 with mass-forming ICCs, 48 (78.7%) had targetoid appearance and 13 (21.3%) hypointense signal. On T2-W sequences, 48 lesions had targetoid appearance while 13 hyperintense signal. After the injection of contrast medium, all lesions showed Rim Arterial Hyperenhancement (APHE), during arterial phase and progressive contrast enhancement with non-peripheral washout appearance in portal phase. In transitional phase and hepatobiliary (EOB) phase 48 mass-forming ICCs showed targetoid appearance and 13 (21.3%) showed hypointense SI (Fig. 5) [12]. They demonstrated that mass-forming ICCs are more likely to exhibit targetoid appearance in T1-W, T2-W and DWI sequences, Rim APHE during arterial phase, progressive contrast enhancement and non-wash-out appearance in portal phase with targetoid appearance (TA) in transitional and hepatobiliary Phase (HB) phase, allowing the differentiation between study group and each other control group [12].

The TA is correlated to central fibrous stroma, which appears as an area of lesser intensity, compared to a more hyperintense peripheral area on T2-W sequences. The presence of this central fibrous stroma also typifies the vascular patterns during the post contrast studies [60, 116].

Dynamic contrast-enhanced (DCE)-MRI

DCE-MRI offers functional informations on perfusion, vessel permeability and extracellular-extravascular space composition by assessing the differences in Signal Intensity (SI) during dynamic contrast studies [117–122]. DCE-MRI can be analysed qualitatively, semi quantitatively and quantitatively. Quantitative analysis comprises the assessment of the pharmacokinetics of an administered contrast medium [117–122]. The largely assessed parameter is the volume transfer constant, K_{trans} . The quantitative method shows several weaknesses as high output flexibility, poor consistency since correlated to several variables and different models used [122]. Qualitative approach (qMRI) is based on time–intensity curve (TIC) visual analysis. The main weakness of this approach is the

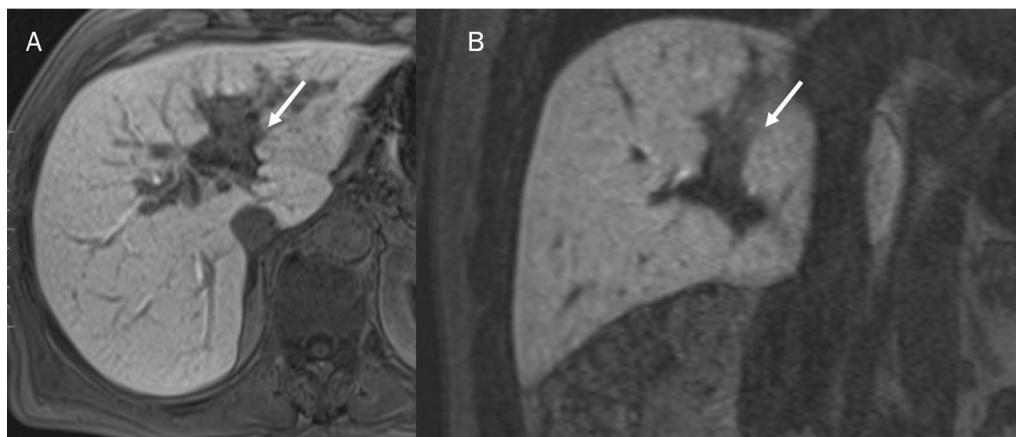


Fig. 5 MRI assessment of ICC in hepatobiliary phase of contrast study. The lesion (arrows) shows hypointense signal intensity in **A** (axial plane) and **B** (coronal plane)

ROI placing [122–130]. Semi-quantitative method evaluates TIC shape parameters offering data on tumour biology [122].

Considering that the liver is a dual-blood-supply organ and that this can affect the quantitative DCE-MRI obtained parameters, however, in ICC patients, it has been demonstrated that pertinent DCE-MRI data can assess angiogenesis, helping diagnosis treatment response evaluation. Tan et al. assessed 50 ICC patients, analysing the rate constant (K_{ep}), extravascular space volume fraction (V_e), and tissue volume transfer constant (K_{trans}). There showed that K_{trans} , K_{ep} , and V_e values were all not correlated with pathological classification [126]. Zhou et al. demonstrated that radiomics signature derived from DCE-MRI can be a consistent biomarker for calculating MVI of ICC [127]. Lin et al. found that kinetic model is a new and feasible method to differentiate HCC from ICC in pre-transplantation setting [128]. Konstantinidis et al. showed that in ICC patients subjected to hepatic arterial chemotherapy infusion, tumour perfusion DCE-MRI parameters were higher in ≥ 3 -year survivors and permitted to distinguish this group from < 3 -year survivors [130].

Diffusion weighted imaging-MRI

DWI provides functional quantitative parameters on the tissue's microstructure valuating water proton mobility. Water diffusion mobility is linked to cell density, vascularity and viscosity of tissues and it's possible to obtain biomarkers employing a mono-exponential or bi-exponential approach [130–142]. Intravoxel Incoherent Motion method (IVIM) is a bi-exponential approach, which allow to obtain the pure tissue coefficient (D_t) linked only to diffusion water mobility, the

pseudo-diffusion coefficient (D_p) linked to blood mobility, and the perfusion fraction (f_p) [143–148]. The conventional DWI method is based on the theory that water diffusion follows a Gaussian motion. However, water molecule diffusion within biologic tissue exhibits non-Gaussian behavior. Jensen et al. in 2005 suggested a non-Gaussian diffusion model named Diffusion Kurtosis imaging (DKI) [149]. Using DKI it is possible to obtain kurtosis median coefficient (MK), which measures the tissue diffusion deviation from a Gaussian model, and the mean value of the diffusion coefficient (MD) with the correction of the non-Gaussian bias [149–151].

The role of DWI in ICC has been evaluated in different studies (Fig. 6). Xu et al. showed that DWI detection rates were higher than those of the morphological sequences alone and there were significant differences between the Apparent Diffusion Coefficient (ADC) values of the lesion edge, lesion centre and liver parenchyma [152]. Kovač et al. demonstrated that univariate analysis shown that several findings suggested ICC diagnosis over metastases: lobulated shape, heterogeneous T2W signal intensity, capsular retraction, segmental biliary dilatation, target sign on DWI and rim-like enhancement on arterial phase followed by progressive enhancement in delayed phases. ADC values measured in the periphery of the lesion were significantly lower in ICC. Multivariate analysis showed that TA on DWI was the most significant predictor of ICC (Fig. 7 and 8) [153]. This result was confirmed by several researches and in differential diagnosis between ICC and HCC, TA was the parameter which allowed it [154–159]. Kovač et al. [155] assessed IVIM-derived parameters, showing that D could help in differentiation between ICC and metastasis. Shao et al. demonstrated that ADC, D ,

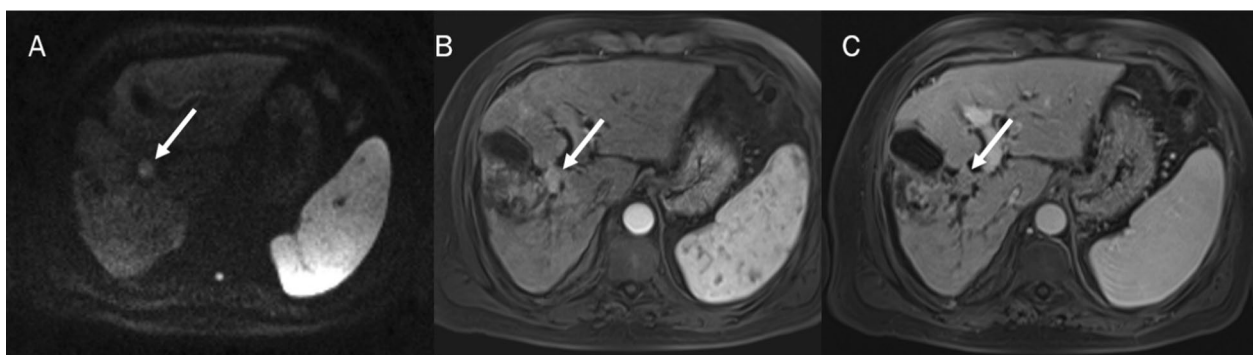


Fig. 6 In DWI (A: b 800 s/mm²) the lesion shows restricted signal and arterial hyperenhancement (B) with progressive enhancement (C) during contrast study

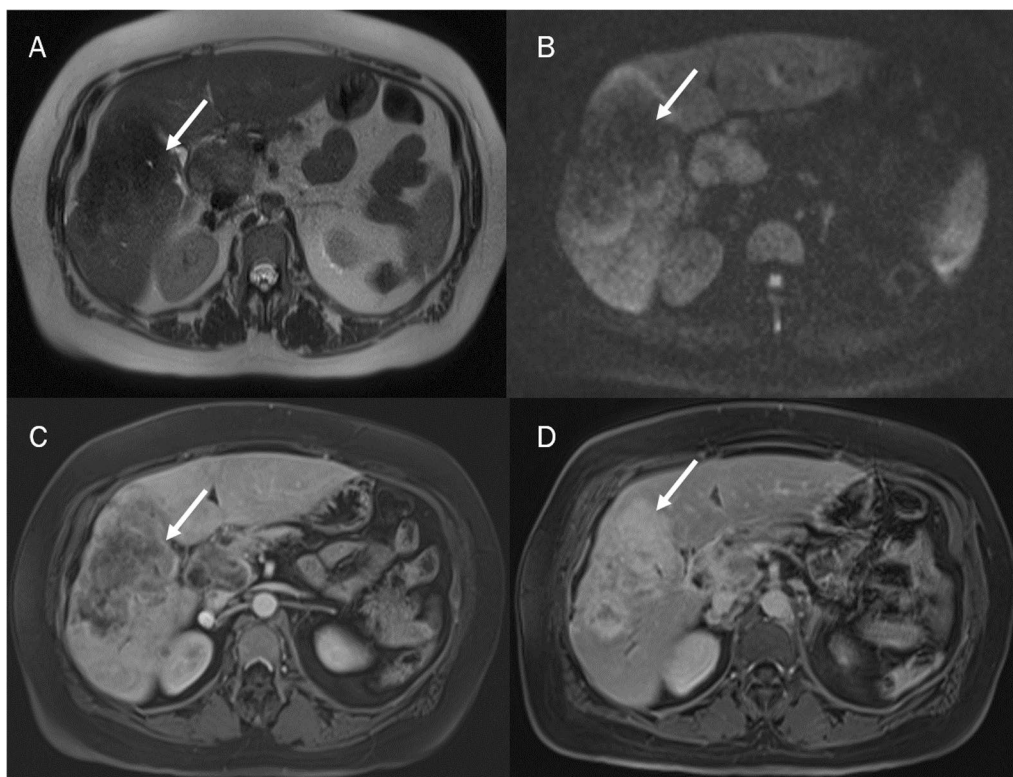


Fig. 7 The targetoid appearance (TA) due to the fibrous stroma in the center of the ICC appears as a central area of less intensity, compared to a more hyperintense peripheral area on T2-W sequences (A) and DWI (B). The presence of this central fibrous stroma also characterizes the behaviour during the dynamic study. On dynamic contrast study, the mass-forming ICCS showed prominent peripheral rim enhancement (C: arterial phase) with centripetal or gradual progressive enhancement (D: delayed phase)

and f values could help ICC from HCC [160]. These results were obtained also by Peng et al., which showed that ADC and D_{slow} were significantly lower in the HCC group than in the ICC group, while D_{fast} was significantly higher in the HCC group than in the ICC group; f did not significantly differ between the HCC and ICC groups [161].

At the best of our knowledge no data on non-Gaussian diffusion behaviour has been described in ICC patients.

BOLD-MRI

Hypoxia is developing key factor of the aggressive tumour biology and the relative resistance to conventional as well as targeted therapies [162]. The only non-invasive



diagnostic tool that could reproduce in clinical setting blood oxygen level is blood oxygen level- dependent (BOLD) functional MRI (fMRI). BOLD MRI makes use of paramagnetic properties of deoxyhemoglobin and is mainly used for regional quantification of oxygenation [162, 163].

To date, only Park et al. assessed BOLD in ICC. They evaluated 100 patients (43 HCCs, 36 metastases, 17 ICCs, and 23 haemangiomas). BOLD MRI was performed using a multiple fast-field echo sequence to generate 20 T2*-W images. The T2* value of each tumour were calculated. They demonstrated that the mean T2* value (ms) of haemangiomas (97.3 ± 20.2) was the highest, followed by HCCs (48.4 ± 12.7), metastases (37.1 ± 10.5), and cholangiocarcinoma's (36.6 ± 11.1). These values were significantly different (haemangioma vs. others tumours and HCC vs. metastasis or cholangiocarcinoma) ($p \leq 0.001$). The agreement between the T2* colour map and dynamic images was moderate for all tumours ($k=0.544$), good for tumours >2.0 cm ($k=0.666$), and fair for tumours ≤ 2.0 cm ($k=0.334$). With the gadoxetic acid-enhanced MRI used as a reference, the sensitivities of BOLD MRI (T2* colour map) for displaying hypervascularity of HCC (categories of 1–3) were 81.0% ($n=34/42$) and 78.6% ($n=33/42$) for both observers [163].

Today, MRI is unique compared to CT and US, since it allows during only one protocol study to assess conventional data, obtained by T2-W and T1-W sequences with functional data, obtained by DWI, DCE-MRI and Bold sequences. In this scenario MRI not only is a problem solving, but the first toll that should be used in patients with FLLs.

Radiomics analysis

Radiomics is a rapidly evolving field of research concerned with the extraction of quantitative data, the so-called radiomic features, within medical images. Radiomic features capture tissue and lesion characteristics such as heterogeneity and shape and may, alone or in

combination with demographic, histologic, genomic, or proteomic data, be used for clinical problem solving [73, 164–175]. Radiomics could hypothetically assist cancer detection, prognosis evaluation, response to treatment assessment, monitoring of disease status [176–179]. Radiomic is planned to be utilised in precision medicine decision support, employing standard of care images that are usually obtained in clinical setting [73, 166–170]. Moreover, Radiomics offers prognostic biomarker which allow for a fast, low-cost, and repeatable means for longitudinal analysis [171–179].

To date, in several studies have been assessed the role of radiomics or radiogenomics in ICC [72, 79, 180–204]. The area of main interest has been the evaluation of recurrence after surgical resection [72, 79, 180–187]. Chu et al. [79] evaluated 203 ICCs, that were allocated with a ratio of 7:3 into the training cohort and the validation cohort. Clinical characteristics and radiomics features were selected using random forest algorithm and logistic models to construct a clinical model and a radiomics model, respectively. The radiomics model showed a higher AUC than the clinical model in the validation cohort for predicting futile resection in ICC. The radiomics model reached a sensitivity of 0.846 and a specificity of 0.771 in the validation cohort. Moreover, the radiomics model had comparable AUCs with the combined model in training and validation cohorts [79]. Quin et al. [180] developed a multilevel model, integrating clinicopathology, molecular pathology and radiology to predict early recurrence after curative surgery, using a machine-learning analysis of 18,120 radiomic features based on CT contrast studies and 48 clinico-radiologic features. They showed that the radiomics-based multilevel model had superior performance to rival models and conventional staging systems, and could serve as a visual prognostic tool to plan surveillance and guide post-operative individualized management [180]. Also Hao et al. [181] developed a non-invasive CT based radiomics analysis model to predict early recurrence in 177 ICC patients.

Radiomic features were extracted on CT images. Six established radiomics models were selected as stable ones by robustness-based rule. Among those models, Max-Relevance Min-Redundancy (MRMR) combined with Gradient Boosting Machine (GBM) yielded the highest AUCs of 0.802 and 0.781 in the training and test cohorts, respectively [181]. Xiang et al. [72] developed a radiomics prediction model based on contrast-enhanced CT to distinguish Microvascular invasion (MVI) in ICCs. Also, Zhou et al. [127] develop a radiomics signature for preoperative prediction of MVI in ICC patients. They evaluated the data obtained based on DCE-MR images.

An area of current interest is the possibility of identifying ideal patients for ablative treatment. Mosconi et al. [182] assessed the relationships between CT textural features prior to TARE and objective response (OR), progression-free survival (PFS), and overall survival (OS). Of the 55 patients, 53 had post-TARE imaging available, showing OR in 56.6% of cases. Texture analysis showed that ICCs showing OR after TARE had a higher uptake of iodine contrast in the arterial phase (higher mean histogram values, $p < 0.001$) and more homogeneous distribution (lower kurtosis, $p = 0.043$; GLCM contrast, $p = 0.004$; GLCM dissimilarity, $p = 0.005$, and higher GLCM homogeneity, $p = 0.005$; and GLCM correlation $p = 0.030$) at the pre-TARE CT scan. A favourable radiomic signature was calculated and observed in 15 of the 55 patients. The median PFS of these 15 patients was 12.1 months and that of the remaining 40 patients was 5.1 months ($p = 0.008$) [182].

Nodal status has also been investigated [196, 197].

The merit of this new tool is that it is able to get digital data from medical imaging and when performed under appropriate protocols, is more robust and reproducible. Nevertheless, there are remaining issues for clinical setting. First, reproducibility is a very important issue. This is correlated to several features, as acquisition protocol, method of segmentation, method for extracting imaging features, and acquisition of clinical and genomic data [102, 198–205].

ICC and Li-RADS: LR-M

The American College of Radiology (ACR) established the Liver Imaging Reporting and Data System (LI-RADS) in patients at risks for HCC in 2011, which has been advanced over multiple updates to version 2018. In 2013, it has been introduced the concept of LR-OM for non-HCC malignancies, which was renamed as LR-M in 2014 [206–217]. Also, ACR introduced the CEUS LI-RADS in 2016 and modified LR-M observations in 2017 [211, 212]. Several researches demonstrated the role of LR-M observations for differentiating non-HCC malignancies from HCCs. An et al. [214] showed that CT and MRI

observations had similar accuracy for discriminating non-HCC malignancies from HCC, with pooled accuracies of 79.9 and 82.4% for categorizing LR-M. Kim et al. [215] showed that non-HCC malignancies could be differentiated from HCCs with a sensitivity of 89% and a specificity of 48% by employing LR-M criteria of v2018 at gadoxetate-enhanced MRI. Zheng et al. [216] assessed that CEUS LI-RADS showed a sensitivity of 89% and a specificity of 88% for LR-M category.

Multiphase contrast studies are required to evaluate LI-RADS features. For therapy-naive lesions submitting to CT, non contrast phase is optional, while it is necessary in the post treatment setting. Late arterial phase is strongly preferred over early arterial phase [217].

CEUS is appropriate as problem solving, classifying observations, and distinguishing tumour in vein from bland thrombus [217–220].

Post-treatment assessment

The primary endpoint of locoregional therapies is to obtain a complete necrosis of liver tumour that is correlated to produce a safety margin of at least 10 mm round the external margin of the tumour. RFA is a hyperthermic method causing necrosis thanks to thermocoagulation. Using RFA, the area of active tissue heating is limited to few millimetres near to electrode, with the residue of the target being heated via thermal conduction [22].

Post-ablation imaging is necessary to assess the efficacy and the safety of the treatment [22], and should be done at programmed times to evaluate response and to detect new lesions so as possible complications. Though there is no usually recognised post-treatment surveillance procedure, it should comprise 1-, 3-, 6-, 9-, and 12-month CT or MRI follow up, as for HCCs [3]. Additionally, post treatment features should be problematic to comprehend considering target location, employed treatment, used response criteria. In this scenario, imaging observations are correlated to the type and the method of therapy delivery, the timing of treatment, and the imaging technique being used to observe the effects [28].

Conclusions

Several morphological and functional data obtained during imaging studies allow a truthful ICC diagnosis. The choice of modality (CT, US/CEUS or MRI) and MRI contrast agent (extracellular or hepatobiliary) is correlated to patient, department, and regional features. MRI allows to correlate morphological and functional data in the ICC assessment. Also, Radiomics is an emerging field in the assessment of ICC patients.

Post treatment imaging is necessary to evaluate the efficacy and the safety of therapies so as patient surveillance. Imaging observations are correlated to the type and the

method of therapy delivery, the timing of treatment, and the imaging technique being used to observe the effects.

Acknowledgements

The authors are grateful to Alessandra Trocino, librarian at the National Cancer Institute of Naples, Italy.

Author contributions

The authors confirm that the article is not under consideration for publication elsewhere. Each author has participated sufficiently to take public responsibility for the manuscript content. All authors read and approved the final manuscript.

Funding

No funding.

Availability of data and materials

The data are available at link <https://zenodo.org/record/6368235#.YkKjNShBy3A>.

Declarations

Ethics approval and consent to participate

Not applicable.

Consent for publication

Not applicable.

Competing interests

The authors declare that they have no competing interests.

Author details

¹Division of Radiology, "Istituto Nazionale Tumori IRCCS Fondazione Pascale – IRCCS di Napoli", 80131 Naples, Italy. ²Medical Oncology Division, Igea SpA, Napoli, Italy. ³Division of Hepatobiliary Surgical Oncology, "Istituto Nazionale Tumori IRCCS Fondazione Pascale – IRCCS di Napoli", 80131 Naples, Italy. ⁴Division of Radiotherapy, "Istituto Nazionale Tumori IRCCS Fondazione Pascale – IRCCS di Napoli", 80131 Naples, Italy. ⁵Department of Diagnostic Imaging, Area of Cardiovascular and Interventional Imaging, Abruzzo Health Unit 1, Milan, Italy. ⁶Italian Society of Medical and Interventional Radiology (SIRM), SIRM Foundation, Milan, Italy. ⁷Diagnostic Imaging Section, University of Aquila, L'Aquila, Italy. ⁸Division of Radiology, "Università Degli Studi Della Campania Luigi Vanvitelli", Naples, Italy. ⁹Division of Abdominal Oncology, "Istituto Nazionale Tumori IRCCS Fondazione Pascale – IRCCS di Napoli", Naples, Italy. ¹⁰Department of Medicine, Surgery and Dentistry, University of Salerno, Salerno, Italy.

Received: 30 January 2022 Accepted: 18 March 2022

Published: 28 March 2022

References

- Sung H, Ferlay J, Siegel RL, Laversanne M, Soerjomataram I, Jemal A, Bray F. Global cancer statistics 2020: GLOBOCAN estimates of incidence and mortality worldwide for 36 cancers in 185 countries. *CA Cancer J Clin*. 2021. <https://doi.org/10.3322/caac.21660>.
- World Health Organization (WHO). Global Health Estimates 2020: Deaths by Cause, Age, Sex, by Country and by Region, 2000–2019. WHO; 2020. Accessed December 11, 2020.
- Granata V, Grassi R, Fusco R, Belli A, Cutolo C, Pradella S, Grazzini G, La Porta M, Brunese MC, De Muzio F, Ottaiano A, Avallone A, Izzo F, Petrillo A. Diagnostic evaluation and ablation treatments assessment in hepatocellular carcinoma. *Infect Agent Cancer*. 2021;16(1):53. <https://doi.org/10.1186/s13027-021-00393-0>.
- Barabino M, Gurgitano M, Fochesato C, Angileri SA, Franceschelli G, Santambrogio R, Mariani NM, Opocher E, Carrafiello G. LI-RADS to categorize liver nodules in patients at risk of HCC: tool or a gadget in daily practice? *Radiol Med*. 2021;126(1):5–13. <https://doi.org/10.1007/s11547-020-01225-8>.
- Cholangiocarcinoma Working Group. Italian Clinical Practice Guidelines on Cholangiocarcinoma—part I: classification, diagnosis and staging. *Dig Liver Dis*. 2020;52(11):1282–93. <https://doi.org/10.1016/j.dld.2020.06.045>.
- Cholangiocarcinoma Working Group. Italian Clinical Practice Guidelines on Cholangiocarcinoma—Part II: treatment. *Dig Liver Dis*. 2020;52(12):1430–42. <https://doi.org/10.1016/j.dld.2020.08.030>.
- Nakanuma Y, Sato Y, Harada K, Sasaki M, Xu J, Ikeda H. Pathological classification of intrahepatic cholangiocarcinoma based on a new concept. *World J Hepatol*. 2010;2:419–27.
- Aishima S, Oda Y. Pathogenesis and classification of intrahepatic cholangiocarcinoma: different characters of perihilar large duct type versus peripheral small duct type. *J Hepatobiliary Pancreat Sci*. 2015;22:94–100.
- Nakanuma Y, Kakuda Y. Pathologic classification of cholangiocarcinoma: new concepts. *Best Pract Res Clin Gastroenterol*. 2015;29:277–93.
- Patrone R, Izzo F, Palaia R, Granata V, Nasti G, Ottaiano A, Pasta G, Belli A. Minimally invasive surgical treatment of intrahepatic cholangiocarcinoma: a systematic review. *World J Gastrointest Oncol*. 2021;13(12):2203–15. <https://doi.org/10.4251/wjgo.v13.i12.2203>.
- Gabelloni M, Di Nasso M, Morganti R, Faggioni L, Masi G, Falcone A, Neri E. Application of the ESR iGuide clinical decision support system to the imaging pathway of patients with hepatocellular carcinoma and cholangiocarcinoma: preliminary findings. *Radiol Med*. 2020;125(6):531–7. <https://doi.org/10.1007/s11547-020-01142-w>.
- Granata V, Grassi R, Fusco R, Setola SV, Belli A, Ottaiano A, Nasti G, La Porta M, Danti G, Cappabianca S, Cutolo C, Petrillo A, Izzo F. Intrahepatic cholangiocarcinoma and its differential diagnosis at MRI: how radiologist should assess MR features. *Radiol Med*. 2021;126(12):1584–600. <https://doi.org/10.1007/s11547-021-01428-7>.
- Granata V, Bicchierai G, Fusco R, Cozzi D, Grazzini G, Danti G, De Muzio F, Maggialelli N, Smorchkova O, D'Elia M, Brunese MC, Grassi R, Giacobbe G, Bruno F, Palumbo P, Grassi F, Brunese L, Grassi R, Miele V, Barile A. Diagnostic protocols in oncology: workup and treatment planning. Part 2: abbreviated MR protocol. *Eur Rev Med Pharmacol Sci*. 2021;25(21):6499–528. https://doi.org/10.26355/eurev_202111_27094.
- Granata V, Fusco R, Amato DM, Albino V, Patrone R, Izzo F, Petrillo A. Beyond the vascular profile: conventional DWI, IVIM and kurtosis in the assessment of hepatocellular carcinoma. *Eur Rev Med Pharmacol Sci*. 2020;24(13):7284–93. https://doi.org/10.26355/eurev_202007_21883.
- Granata V, Fusco R, Maio F, Avallone A, Nasti G, Palaia R, Albino V, Grassi R, Izzo F, Petrillo A. Qualitative assessment of EOB-GD-DTPA and Gd-BT-DO3A MR contrast studies in HCC patients and colorectal liver metastases. *Infect Agent Cancer*. 2019;14:40. <https://doi.org/10.1186/s13027-019-0264-3>.
- Gatti M, Calandri M, Bergamasco L, Darvizeh F, Grazioli L, Inchingolo R, Ippolito D, Rousset S, Veltri A, Fonio P, Faletti R. Characterization of the arterial enhancement pattern of focal liver lesions by multiple arterial phase magnetic resonance imaging: comparison between hepatocellular carcinoma and focal nodular hyperplasia. *Radiol Med*. 2020;125(4):348–55. <https://doi.org/10.1007/s11547-019-01127-4>.
- Orlacchio A, Chegai F, Roma S, Merolla S, Bosa A, Francioso S. Degradable starch microspheres transarterial chemoembolization (DSMs-TACE) in patients with unresectable hepatocellular carcinoma (HCC): long-term results from a single-center 137-patient cohort prospective study. *Radiol Med*. 2020;125(1):98–106. <https://doi.org/10.1007/s11547-019-01093-x>.
- Granata V, Fusco R, Avallone A, Catalano O, Filice F, Leongito M, Palaia R, Izzo F, Petrillo A. Major and ancillary magnetic resonance features of LI-RADS to assess HCC: an overview and update. *Infect Agent Cancer*. 2017;12:23. <https://doi.org/10.1186/s13027-017-0132-y>.
- Granata V, Fusco R, Avallone A, Filice F, Tatangelo F, Piccirillo M, Grassi R, Izzo F, Petrillo A. Critical analysis of the major and ancillary imaging features of LI-RADS on 127 proven HCCs evaluated with functional and morphological MRI: lights and shadows. *Oncotarget*. 2017;8(31):51224–37. <https://doi.org/10.18632/oncotarget.17227>.

20. Granata V, Fusco R, Filice S, Incollongo P, Belli A, Izzo F, Petrillo A. Comment on "State of the art in magnetic resonance imaging of hepatocellular carcinoma": the role of DWI. *Radiol Oncol*. 2019;53(3):369–70. <https://doi.org/10.2478/raon-2019-0031>.
21. Granata V, Fusco R, Filice S, Catalano O, Piccirillo M, Palaia R, Izzo F, Petrillo A. The current role and future perspectives of functional parameters by diffusion weighted imaging in the assessment of histologic grade of HCC. *Infect Agent Cancer*. 2018;13:23. <https://doi.org/10.1186/s13027-018-0194-5>.
22. Izzo F, Granata V, Grassi R, Fusco R, Palaia R, Delrio P, Carrafiello G, Azoulay D, Petrillo A, Curley SA. Radiofrequency ablation and microwave ablation in liver tumors: an update. *Oncologist*. 2019;24(10):e990–1005. <https://doi.org/10.1634/theoncologist.2018-0337>.
23. Wu L, Tsilimigras DI, Farooq A, et al. Potential survival benefit of radiofrequency ablation for small solitary intrahepatic cholangiocarcinoma in nonsurgically managed patients: a population-based analysis. *J Surg Oncol*. 2019;120:1358–64.
24. Yousaf A, Kim JU, Eliahoo J, et al. Ablative therapy for unresectable intrahepatic cholangiocarcinoma: a systematic review and meta-analysis. *J Clin Exp Hepatol*. 2019;9:740–8.
25. Granata V, Palaia R, Albino V, Piccirillo M, Venanzio Setola S, Petrillo A, Izzo F. Electrochemotherapy of cholangiocellular carcinoma at hepatic hilum: a case report. *Eur Rev Med Pharmacol Sci*. 2020;24(12):7051–7. https://doi.org/10.26355/eurrev_202006_21698.
26. De Filippo M, Ziglioli F, Russo U, Pagano P, Brunese L, Bertelli E, Pagnini F, Maestroni U. Radiofrequency ablation (RFA) of T1a renal cancer with externally cooled multined expandable electrodes. *Radiol Med*. 2020;125(8):790–7. <https://doi.org/10.1007/s11547-020-01175-1>.
27. Arrigoni F, Bruno F, Gianneramo C, Palumbo P, Zugaro L, Zoccali C, Barile A, Masciocchi C. Evolution of the imaging features of osteoid osteoma treated with RFA or MRgFUS during a long-term follow-up: a pictorial review with clinical correlations. *Radiol Med*. 2020;125(6):578–84. <https://doi.org/10.1007/s11547-020-01134-w>.
28. Granata V, Grassi R, Fusco R, Setola SV, Palaia R, Belli A, Miele V, Brunese L, Grassi R, Petrillo A, Izzo F. Assessment of ablation therapy in pancreatic cancer: the radiologist's challenge. *Front Oncol*. 2020;10:560952. <https://doi.org/10.3389/fonc.2020.560952>.
29. Granata V, Grassi R, Fusco R, Belli A, Palaia R, Carrafiello G, Miele V, Grassi R, Petrillo A, Izzo F. Local ablation of pancreatic tumors: State of the art and future perspectives. *World J Gastroenterol*. 2021;27(23):3413–28. <https://doi.org/10.3748/wjg.v27.i23.3413>.
30. Catalano O, Sandomenico F, Vallone P, Setola SV, Granata V, Fusco R, Las-toria S, Mansi L, Petrillo A. Contrast-enhanced ultrasound in the assessment of patients with indeterminate abdominal findings at positron emission tomography imaging. *Ultrasound Med Biol*. 2016;42(11):2717–23. <https://doi.org/10.1016/j.ultrasmedbio.2016.06.023>.
31. Mitrea D, Badea R, Mitrea P, Brad S, Nedevschi S. Hepatocellular carcinoma automatic diagnosis within CEUS and B-mode ultrasound images using advanced machine learning methods. *Sensors (Basel)*. 2021;21(6):2202. <https://doi.org/10.3390/s21062202>.
32. Trombadori CML, D'Angelo A, Ferrara F, Santoro A, Belli P, Manfredi R. Radial Scar: a management dilemma. *Radiol Med*. 2021. <https://doi.org/10.1007/s11547-021-01344-w>.
33. Argalia G, Tarantino G, Ventura C, Campioni D, Tagliati C, Guardati P, Kostandini A, Marzoni M, Giuseppetti GM, Giovagnoni A. Shear wave elastography and transient elastography in HCV patients after direct-acting antivirals. *Radiol Med*. 2021. <https://doi.org/10.1007/s11547-020-01326-4>.
34. Ierardi AM, Galbazzi N, Tuttolomondo D, Fusco S, La Mura V, Peyvandi F, Aliberti S, Blasi F, Cozzi D, Carrafiello G, De Filippo M. Deep vein thrombosis in COVID-19 patients in general wards: prevalence and association with clinical and laboratory variables. *Radiol Med*. 2021;126(5):722–8. <https://doi.org/10.1007/s11547-020-01312-w>.
35. Fanelli F, Cannavale A, Chisci E, Citone M, Falcone GM, Michelagnoli S, Miele V. Direct percutaneous embolization of aneurysm sac: a safe and effective procedure to treat post-EVAR type II endoleaks. *Radiol Med*. 2021;126(2):258–63. <https://doi.org/10.1007/s11547-020-01247-2>.
36. Trimboli P, Castellana M, Virili C, Havre RF, Bini F, Marinozzi F, D'Ambrosio F, Giorgino F, Giovannella L, Prosch H, Grani G, Radzina M, Cantisani V. Performance of contrast-enhanced ultrasound (CEUS) in assessing thyroid nodules: a systematic review and meta-analysis using histological standard of reference. *Radiol Med*. 2020;125(4):406–15. <https://doi.org/10.1007/s11547-019-01129-2>.
37. Patrone R, Granata V, Belli A, Palaia R, Albino V, Piccirillo M, Fusco R, Tatangelo F, Nasti G, Avallone A, Izzo F. The safety and efficacy of Glubran 2 as biliostatic agent in liver resection. *Infect Agent Cancer*. 2021;16(1):19. <https://doi.org/10.1186/s13027-021-00358-3>.
38. Granata V, Fusco R, Setola SV, Avallone A, Palaia R, Grassi R, Izzo F, Petrillo A. Radiological assessment of secondary biliary tree lesions: an update. *J Int Med Res*. 2020;48(6):300060519850398. <https://doi.org/10.1177/0300060519850398>.
39. Granata V, Fusco R, Catalano O, Avallone A, Palaia R, Botti G, Tatangelo F, Granata F, Cascella M, Izzo F, Petrillo A. Diagnostic accuracy of magnetic resonance, computed tomography and contrast enhanced ultrasound in radiological multimodality assessment of peribiliary liver metastases. *PLoS ONE*. 2017;12(6):e0179951. <https://doi.org/10.1371/journal.pone.0179951>.
40. Hu HT, Wang W, Chen LD, Ruan SM, Chen SL, Li X, Lu MD, Xie XY, Kuang M. Artificial intelligence assists identifying malignant versus benign liver lesions using contrast-enhanced ultrasound. *J Gastroenterol Hepatol*. 2021. <https://doi.org/10.1111/jgh.15522>.
41. Chammas MC, Bordini AL. Contrast-enhanced ultrasonography for the evaluation of malignant focal liver lesions. *Ultrasonography*. 2022;41(1):4–24. <https://doi.org/10.14366/usg.21001>.
42. Chen Y, Zhu Y, Chen K, Wang H, Zhang W, Bao J, Wang W. Differentiation between hepatocellular carcinoma and intrahepatic cholangiocarcinoma using contrast-enhanced ultrasound: A systematic review and meta-analysis. *Clin Hemorheol Microcirc*. 2021;79(2):293–309. <https://doi.org/10.3233/CH-211145>.
43. Xian MF, Huang Y, Xie WX, Pan KM, Zeng D, Huang H, Li MD, Xie XY, Kuang M, Lu MD, Chen LD, Wang W. LR-M observations on contrast-enhanced ultrasound: detection of hepatocellular carcinoma using additional features in comparison with current LI-RADS criteria. *AJR Am J Roentgenol*. 2021. <https://doi.org/10.2214/AJR.21.26837>.
44. Guo HL, Zheng X, Cheng MQ, Zeng D, Huang H, Xie XY, Lu MD, Kuang M, Wang W, Xian MF, Chen LD. Contrast-Enhanced Ultrasound for Differentiation Between Poorly Differentiated Hepatocellular Carcinoma and Intrahepatic Cholangiocarcinoma. *J Ultrasound Med*. 2021. <https://doi.org/10.1002/jum.15812>.
45. Li R, Yuan MX, Ma KS, Li XW, Tang CL, Zhang XH, et al. Detailed analysis of temporal features on contrast enhanced ultrasound may help differentiate intrahepatic cholangiocarcinoma from hepatocellular carcinoma in cirrhosis. *PLoS ONE*. 2014;9(5):e98612. <https://doi.org/10.1371/journal.pone.0098612>.
46. Li F, Li Q, Liu YB, Han J, Zheng W, Huang YN, et al. Distinguishing intrahepatic cholangiocarcinoma from hepatocellular carcinoma in patients with and without risks: the evaluation of the LR-M criteria of contrast-enhanced ultrasound liver imaging reporting and data system version 2017. *Eur Radiol*. 2019;30(1):461–70. <https://doi.org/10.1007/s00330-019-06317-2>.
47. Chen LD, Ruan SM, Lin Y, Liang JY, Shen SL, Hu HT, et al. Comparison between M-score and LR-M in the reporting system of contrast-enhanced ultrasound LI-RADS. *Eur Radiol*. 2018;29(8):4249–57. <https://doi.org/10.1007/s00330-018-5927-8>.
48. Wildner D, Bernatik T, Greis C, Seitz K, Neurath MF, Strobel D. CEUS in hepatocellular carcinoma and intrahepatic cholangiocellular carcinoma in 320 patients - early or late washout matters: a subanalysis of the DEGUM multicenter trial. *Ultraschall Med*. 2015;36(2):132–9. <https://doi.org/10.1055/s-0034-1399147>.
49. Shin SK, Choi DJ, Kim JH, Kim YS, Kwon OS. Characteristics of contrast-enhanced ultrasound in distinguishing small (<=3 cm) hepatocellular carcinoma from intrahepatic cholangiocarcinoma. *Medicine (Baltimore)*. 2018;97(41):e12781. <https://doi.org/10.1097/md.00000000000012781>.
50. Liu GJ, Wang W, Lu MD, Xie XY, Xu HX, Xu ZF, et al. Contrast-enhanced ultrasound for the characterization of hepatocellular carcinoma and intrahepatic cholangiocarcinoma. *Liver Cancer*. 2015;4(4):241–52. <https://doi.org/10.1159/000367738>.
51. Han J, Liu Y, Han F, Li Q, Yan C, Zheng W, et al. The degree of contrast washout on contrast-enhanced ultrasound in distinguishing intrahepatic cholangiocarcinoma from hepatocellular carcinoma. *Ultrasound*

- Med Biol. 2015;41(12):3088–95. <https://doi.org/10.1016/j.ultrasmedbio.2015.08.001>.
52. Huang JY, Li JW, Ling WW, Li T, Luo Y, Liu JB, et al. Can contrast enhanced ultrasound differentiate intrahepatic cholangiocarcinoma from hepatocellular carcinoma? *World J Gastroenterol*. 2020;26(27):3938–51. <https://doi.org/10.3748/wjg.v26.i27.3938>.
 53. Joo I, Lee JM, Yoon JH. Imaging diagnosis of intrahepatic and perihilar cholangiocarcinoma: recent advances and challenges. *Radiology*. 2018;288(1):7–13. <https://doi.org/10.1148/radiol.2018171187>.
 54. Peng JB, Peng YT, Lin P, Wan D, Qin H, Li X, Wang XR, He Y, Yang H. Differentiating infected focal liver lesions from malignant mimickers: value of ultrasound-based radiomics. *Clin Radiol*. 2021;S0009–9260(21):00486–94. <https://doi.org/10.1016/j.crad.2021.10.009>.
 55. Zhang G, Liu D. Comparative the clinical value of contrast-enhanced ultrasonography, enhancement CT and MRI for diagnosing of liver lesions. *Clin Hemorheol Microcirc*. 2021. <https://doi.org/10.3233/CH-211142>.
 56. Franken LC, Coelen RJS, Erdmann JI, Verheij J, Kop MP, van Gulik TM, Phoa SS. Multidetector computed tomography assessment of vascular involvement in perihilar cholangiocarcinoma. *Quant Imaging Med Surg*. 2021;11(11):4514–21. <https://doi.org/10.21037/qims-20-1303>.
 57. Kim YY, Yeom SK, Shin H, Choi SH, Rhee H, Park JH, Cho ES, Park S, Lee SS, Park MS. Clinical staging of mass-forming intrahepatic cholangiocarcinoma: computed tomography versus magnetic resonance imaging. *Hepatol Commun*. 2021;5(12):2009–18. <https://doi.org/10.1002/hep4.1774>.
 58. Ichikawa S, Yamamoto H, Morita T. Comparison of a Bayesian estimation algorithm and singular value decomposition algorithms for 80-detector row CT perfusion in patients with acute ischemic stroke. *Radiol Med*. 2021;126(6):795–803. <https://doi.org/10.1007/s11547-020-01316-6>.
 59. Rampado O, Depaoli A, Marchisio F, Gatti M, Racine D, Ruggeri V, Ruggirello I, Darvizeh F, Fonio P, Popolo R. Effects of different levels of CT iterative reconstruction on low-contrast detectability and radiation dose in patients of different sizes: an anthropomorphic phantom study. *Radiol Med*. 2021;126(1):55–62. <https://doi.org/10.1007/s11547-020-01228-5>.
 60. Shin N, Choi JA, Choi JM, Cho ES, Kim JH, Chung JJ, Yu JS. Sclerotic changes of cavernous hemangioma in the cirrhotic liver: long-term follow-up using dynamic contrast-enhanced computed tomography. *Radiol Med*. 2020;125(12):1225–32. <https://doi.org/10.1007/s11547-020-01221-y>.
 61. Bottari A, Silipigni S, Carerj ML, Cattafi A, Maimone S, Marino MA, Mazziotti S, Pitrone A, Squadrito G, Ascenti G. Dual-source dual-energy CT in the evaluation of hepatic fractional extracellular space in cirrhosis. *Radiol Med*. 2020;125(1):7–14. <https://doi.org/10.1007/s11547-019-01089-7>.
 62. Cao SE, Zhang LQ, Kuang SC, Shi WQ, Hu B, Xie SD, Chen YN, Liu H, Chen SM, Jiang T, Ye M, Zhang HX, Wang J. Multiphase convolutional dense network for the classification of focal liver lesions on dynamic contrast-enhanced computed tomography. *World J Gastroenterol*. 2020;26(25):3660–72. <https://doi.org/10.3748/wjg.v26.i25.3660>.
 63. Asayama Y, Yoshimitsu K, Irie H, Tajima T, Nishie A, Hirakawa M, Nakayama T, Kakiyama D, Taketomi A, Aishima S, Honda H. Delayed-phase dynamic CT enhancement as a prognostic factor for mass-forming intrahepatic cholangiocarcinoma. *Radiology*. 2006;238(1):150–5. <https://doi.org/10.1148/radiol.2381041765>.
 64. Granata V, Fusco R, Bicchierai G, Cozzi D, Grazzini G, Danti G, De Muzio F, Maggialelli N, Smorchkova O, D'Elia M, Brunese MC, Grassi R, Giacobbe G, Bruno F, Palumbo P, Lacasella GV, Brunese L, Grassi R, Miele V, Barile A. Diagnostic protocols in oncology: workup and treatment planning. Part 1: the optimization of CT protocol. *Eur Rev Med Pharmacol Sci*. 2021;25(22):6972–94. https://doi.org/10.26355/eurrev_2021_11_27246.
 65. Cicero G, Mazziotti S, Silipigni S, Blandino A, Cantisani V, Pergolizzi S, D'Angelo T, Stagno A, Maimone S, Squadrito G, Ascenti G. Dual-energy CT quantification of fractional extracellular space in cirrhotic patients: comparison between early and delayed equilibrium phases and correlation with oesophageal varices. *Radiol Med*. 2021. <https://doi.org/10.1007/s11547-021-01341-z>.
 66. Granata V, Fusco R, de Lutio di Castelguidone E, Avallone A, Palaia R, Delrio P, Tatangelo F, Botti G, Grassi R, Izzo F, Petrillo A. Diagnostic performance of gadoteric acid-enhanced liver MRI versus multidetector CT in the assessment of colorectal liver metastases compared to hepatic resection. *BMC Gastroenterol*. 2019;19(1):129. <https://doi.org/10.1186/s12876-019-1036-7>.
 67. Agostini A, Borgheresi A, Mari A, Floridi C, Bruno F, Carotti M, Schicchi N, Barile A, Maggi S, Giovagnoni A. Dual-energy CT: theoretical principles and clinical applications. *Radiol Med*. 2019;124(12):1281–95. <https://doi.org/10.1007/s11547-019-01107-8>.
 68. Cereser L, Girometti R, Da Re J, Marchesini F, Como G, Zuiani C. Inter-reader agreement of high-resolution computed tomography findings in patients with COVID-19 pneumonia: a multi-reader study. *Radiol Med*. 2021;126(4):577–84. <https://doi.org/10.1007/s11547-020-01320-w>.
 69. Okamura T, Yamada Y, Yamada M, Yamazaki A, Shiraga N, Jinzaki M. Image quality of virtual monochromatic images obtained using 320-detector row CT: a phantom study evaluating the effects of iterative reconstruction and body size. *Eur J Radiol*. 2017;95:212–21. <https://doi.org/10.1016/j.ejrad.2017.08.016>.
 70. Galassi M, Iavarone M, Rossi S, Bota S, Vavassori S, Rosa L, Leoni S, Venerandi L, Marinelli S, Sangiovanni A, Veronese L, Fraquelli M, Granito A, Golfieri R, Colombo M, Bolondi L, Piscaglia F. Patterns of appearance and risk of misdiagnosis of intrahepatic cholangiocarcinoma in cirrhosis at contrast enhanced ultrasound. *Liver Int*. 2013;33(5):771–9. <https://doi.org/10.1111/liv.12124>.
 71. Chen LD, Xu HX, Xie XY, Lu MD, Xu ZF, Liu GJ, Liang JY, Lin MX. Enhancement patterns of intrahepatic cholangiocarcinoma: comparison between contrast-enhanced ultrasound and contrast-enhanced CT. *Br J Radiol*. 2008;81(971):881–9. <https://doi.org/10.1259/bjr/22318475>.
 72. Xiang F, Wei S, Liu X, Liang X, Yang L, Yan S. Radiomics analysis of contrast-enhanced CT for the preoperative prediction of microvascular invasion in mass-forming intrahepatic cholangiocarcinoma. *Front Oncol*. 2021;11:774117. <https://doi.org/10.3389/fonc.2021.774117>.
 73. Gurgitano M, Angileri SA, Rodà GM, Liguori A, Pandolfi M, Ierardi AM, Wood BJ, Carrafiello G. Interventional Radiology ex-machina: impact of Artificial Intelligence on practice. *Radiol Med*. 2021;126(7):998–1006. <https://doi.org/10.1007/s11547-021-01351-x>.
 74. Ponnoprat D, Inkeaw P, Chaijaruwanchit J, Traisathit P, Sripan P, Inmutto N, Na Chiangmai W, Pongnikorn D, Chitapanarux I. Classification of hepatocellular carcinoma and intrahepatic cholangiocarcinoma based on multi-phase CT scans. *Med Biol Eng Comput*. 2020;58(10):2497–515. <https://doi.org/10.1007/s11517-020-02229-2>.
 75. Tsunematsu S, Chuma M, Kamiyama T, Miyamoto N, Yabusaki S, Hatanaka K, Mitsuhashi T, Kamachi H, Yokoo H, Kakisaka T, Tsuruga Y, Orimo T, Wakayama K, Ito J, Sato F, Terashita K, Nakai M, Tsukuda Y, Sho T, Suda G, Morikawa K, Natsuzaka M, Nakanishi M, Ogawa K, Taketomi A, Matsuno Y, Sakamoto N. Intratumoral artery on contrast-enhanced computed tomography imaging: differentiating intrahepatic cholangiocarcinoma from poorly differentiated hepatocellular carcinoma. *Abdom Imaging*. 2015;40(6):1492–9. <https://doi.org/10.1007/s00261-015-0352-9>.
 76. Zhao YJ, Chen WX, Wu DS, Zhang WY, Zheng LR. Differentiation of mass-forming intrahepatic cholangiocarcinoma from poorly differentiated hepatocellular carcinoma: based on the multivariate analysis of contrast-enhanced computed tomography findings. *Abdom Radiol (NY)*. 2016;41(5):978–89. <https://doi.org/10.1007/s00261-015-0629-z>.
 77. Ruys AT, van Beem BE, Engelbrecht MR, Bipat S, Stoker J, Van Gulik TM. Radiological staging in patients with hilar cholangiocarcinoma: a systematic review and meta-analysis. *Br J Radiol*. 2012;85(1017):1255–62.
 78. Ichikawa S, Isoda H, Shimizu T, Tamada D, Taura K, Togashi K, Onishi H, Motosugi U. Distinguishing intrahepatic mass-forming biliary carcinomas from hepatocellular carcinoma by computed tomography and magnetic resonance imaging using the Bayesian method: a bi-center study. *Eur Radiol*. 2020;30(11):5992–6002. <https://doi.org/10.1007/s00330-020-06972-w>.
 79. Chu H, Liu Z, Liang W, Zhou Q, Zhang Y, Lei K, Tang M, Cao Y, Chen S, Peng S, Kuang M. Radiomics using CT images for preoperative prediction of futile resection in intrahepatic cholangiocarcinoma. *Eur Radiol*. 2021;31(4):2368–76. <https://doi.org/10.1007/s00330-020-07250-5>.
 80. Megibow AJ. Clinical abdominal dual-energy CT: 15 years later. *Abdom Radiol (NY)*. 2020;45(4):198–201. <https://doi.org/10.1007/s00261-019-02250-6>.
 81. Schicchi N, Fogante M, Palumbo P, Agliata G, Esposito Pirani P, Di Cesare E, Giovagnoni A. The sub-millisievert era in CTCA: the technical basis of

- the new radiation dose approach. *Radiol Med.* 2020;125(11):1024–39. <https://doi.org/10.1007/s11547-020-01280-1>.
82. Agostini A, Borgheresi A, Carotti M, Ottaviani L, Badaloni M, Floridi C, Giovagnoni A. Third-generation iterative reconstruction on a dual-source, high-pitch, low-dose chest CT protocol with tin filter for spectral shaping at 100 kV: a study on a small series of COVID-19 patients. *Radiol Med.* 2021;126(3):388–98. <https://doi.org/10.1007/s11547-020-01298-5>.
 83. Park SH, Kim YS, Choi J. Dosimetric analysis of the effects of a temporary tissue expander on the radiotherapy technique. *Radiol Med.* 2021;126(3):437–44. <https://doi.org/10.1007/s11547-020-01297-6>.
 84. Nakamura Y, Higaki T, Honda Y, Tatsugami F, Tani C, Fukumoto W, Narita K, Kondo S, Akagi M, Awai K. Advanced CT techniques for assessing hepatocellular carcinoma. *Radiol Med.* 2021;126(7):925–35. <https://doi.org/10.1007/s11547-021-01366-4>.
 85. Cozzi D, Moroni C, Cavigli E, Bindi A, Caviglioli C, Nazerian P, Vanni S, Miele V, Bartolucci M. Prognostic value of CT pulmonary angiography parameters in acute pulmonary embolism. *Radiol Med.* 2021;126(8):1030–6. <https://doi.org/10.1007/s11547-021-01364-6>.
 86. Brizi MG, Perillo F, Cannone F, Tuzza L, Manfredi R. The role of imaging in acute pancreatitis. *Radiol Med.* 2021;126(8):1017–29. <https://doi.org/10.1007/s11547-021-01359-3>.
 87. Assadsangabi R, Babaei R, Songco C, Ivanovic V, Bobinski M, Chen YJ, Nabavizadeh SA. Multimodality oncologic evaluation of superficial neck and facial lymph nodes. *Radiol Med.* 2021;126(8):1074–84. <https://doi.org/10.1007/s11547-021-01367-3>.
 88. Granata V, Grassi R, Fusco R, Galdiero R, Setola SV, Palaia R, Belli A, Silvestro L, Cozzi D, Brunese L, Petrillo A, Izzo F. Pancreatic cancer detection and characterization: state of the art and radiomics. *Eur Rev Med Pharmacol Sci.* 2021;25(10):3684–99. https://doi.org/10.26355/eurrev_202105_25935.
 89. Granata V, Fusco R, Catalano O, Setola SV, de Lutio di Castelguidone E, Piccirillo M, Palaia R, Grassi R, Granata F, Izzo F, Petrillo A. Multidetector computer tomography in the pancreatic adenocarcinoma assessment: an update. *Infect Agent Cancer.* 2016;11:57. <https://doi.org/10.1186/s13027-016-0105-6>.
 90. Bertocchi E, Barugola G, Nicosia L, Mazzola R, Ricchetti F, Dell'Abate P, Alongi F, Ruffo G. A comparative analysis between radiation dose intensification and conventional fractionation in neoadjuvant locally advanced rectal cancer: a monocentric prospective observational study. *Radiol Med.* 2020;125:990–8. <https://doi.org/10.1007/s11547-020-01189-9>.
 91. Agostini A, Floridi C, Borgheresi A, Badaloni M, Esposito Pirani P, Terilli F, Ottaviani L, Giovagnoni A. Proposal of a low-dose, long-pitch, dual-source chest CT protocol on third-generation dual-source CT using a tin filter for spectral shaping at 100 kVp for Coronavirus Disease 2019 (COVID-19) patients: a feasibility study. *Radiol Med.* 2020;125:365–73. <https://doi.org/10.1007/s11547-020-01179-x>.
 92. Cicero G, Ascenti G, Albrecht MH, Blandino A, Cavallaro M, D'Angelo T, Carerj ML, Vogl TJ, Mazziotti S. Extra-abdominal dual-energy CT applications: a comprehensive overview. *Radiol Med.* 2020;125:384–97. <https://doi.org/10.1007/s11547-019-01126-5>.
 93. Yoon JH, Chang W, Lee ES, Lee SM, Lee JM. Double low-dose dual-energy liver CT in patients at high-risk of HCC: a prospective, randomized. *Single-Center Study Invest Radiol.* 2020;55(6):340–8. <https://doi.org/10.1097/RLI.0000000000000643>.
 94. Joob B, Wiwanitkit V. Cholangiocarcinoma versus small liver abscess in dual source dual-energy CT quantitative parameters. *Eur J Radiol.* 2018;99:130. <https://doi.org/10.1016/j.ejrad.2017.12.022>.
 95. Kim JE, Kim HO, Bae K, Cho JM, Choi HC, Choi DS. Differentiation of small intrahepatic mass-forming cholangiocarcinoma from small liver abscess by dual source dual-energy CT quantitative parameters. *Eur J Radiol.* 2017;92:145–52. <https://doi.org/10.1016/j.ejrad.2017.05.012>.
 96. Pang G, Shao C, Lv Y, Zhao F. Tumor attenuation and quantitative analysis of perfusion parameters derived from triphasic CT scans in hepatocellular carcinoma: relationship with histological grade. *Medicine (Baltimore).* 2021;100(16):e25627. <https://doi.org/10.1097/MD.00000000000025627>.
 97. Perl RM, Portugal J, Hinterleitner C, Hinterleitner M, Kloth C, Walter SS, Bitzer M, Horger MS. Differences between CT-perfusion and biphasic contrast-enhanced CT for detection and characterization of hepatocellular carcinoma: potential explanations for discrepant cases. *Anticancer Res.* 2021;41(3):1451–8. <https://doi.org/10.21873/anticancer.14903>.
 98. Zhao F, Pang G, Li X, Yang S, Zhong H. Value of perfusion parameters histogram analysis of triphasic CT in differentiating intrahepatic mass forming cholangiocarcinoma from hepatocellular carcinoma. *Sci Rep.* 2021;11(1):23163. <https://doi.org/10.1038/s41598-021-02667-4>.
 99. Bozkurt M, Eldem G, Bozbulut UB, Bozkurt MF, Kılıçkap S, Peynircioğlu B, Çil B, Lay Ergün E, Volkan-Salanci B. Factors affecting the response to Y-90 microsphere therapy in the cholangiocarcinoma patients. *Radiol Med.* 2021;126(2):323–33. <https://doi.org/10.1007/s11547-020-01240-9>.
 100. Kim BH, Kim JS, Kim KH, Moon HJ, Kim S. Clinical significance of radiation dose-volume parameters and functional status on the patient-reported quality of life changes after thoracic radiotherapy for lung cancer: a prospective study. *Radiol Med.* 2021;126(3):466–73. <https://doi.org/10.1007/s11547-020-01273-0>.
 101. Mathew RP, Sam M, Raubenheimer M, Patel V, Low G. Hepatic hemangiomas: the various imaging avatars and its mimickers. *Radiol Med.* 2020;125(9):801–15. <https://doi.org/10.1007/s11547-020-01185-z>.
 102. Granata V, Fusco R, Avallone A, De Stefano A, Ottaviano A, Sbordone C, Brunese L, Izzo F, Petrillo A. Radiomics-derived data by contrast enhanced magnetic resonance in RAS mutations detection in colorectal liver metastases. *Cancers (Basel).* 2021;13(3):453. <https://doi.org/10.3390/cancers13030453>.
 103. Esposito A, Buscarino V, Raciti D, Casiraghi E, Manini M, Biondetti P, Forzenigo L. Characterization of liver nodules in patients with chronic liver disease by MRI: performance of the Liver Imaging Reporting and Data System (LI-RADS vol 2018) scale and its comparison with the Likert scale. *Radiol Med.* 2020;125(1):15–23. <https://doi.org/10.1007/s11547-019-01092-y>.
 104. Orsatti G, Zucchetto P, Varotto A, Crimi F, Weber M, Cecchin D, Bisogno G, Spimpolo A, Giraudo C, Stramare R. Volumetric histograms-based analysis of apparent diffusion coefficients and standard uptake values for the assessment of pediatric sarcoma at staging: preliminary results of a PET/MRI study. *Radiol Med.* 2021. <https://doi.org/10.1007/s11547-021-01340-0>.
 105. Fusco R, Granata V, Petrillo A. Introduction to special issue of radiology and imaging of cancer. *Cancers (Basel).* 2020;12(9):2665. <https://doi.org/10.3390/cancers12092665>.
 106. Granata V, Fusco R, Venanzio Setola S, Mattace Raso M, Avallone A, De Stefano A, Nasti G, Palaia R, Delrio P, Petrillo A, Izzo F. Liver radiologic findings of chemotherapy-induced toxicity in liver colorectal metastases patients. *Eur Rev Med Pharmacol Sci.* 2019;23(22):9697–706. https://doi.org/10.26355/eurrev_201911_19531.
 107. Granata V, Fusco R, Setola SV, Castelguidone ELD, Camera L, Tafuto S, Avallone A, Belli A, Incollingo P, Palaia R, Izzo F, Petrillo A. The multidisciplinary team for gastroenteropancreatic neuroendocrine tumours: the radiologist's challenge. *Radiol Oncol.* 2019;53(4):373–87. <https://doi.org/10.2478/raon-2019-0040>.
 108. Berardo S, Sukhovei L, Andorno S, Carriero A, Stecco A. Quantitative bone marrow magnetic resonance imaging through apparent diffusion coefficient and fat fraction in multiple myeloma patients. *Radiol Med.* 2021;126(3):445–52. <https://doi.org/10.1007/s11547-020-01258-z>.
 109. Crimi F, Capelli G, Spolverato G, Bao QR, Florio A, Milite Rossi S, Cecchin D, Albertoni L, Campi C, Pucciarelli S, Stramare R. MRI T2-weighted sequences-based texture analysis (TA) as a predictor of response to neoadjuvant chemo-radiotherapy (nCRT) in patients with locally advanced rectal cancer (LARC). *Radiol Med.* 2020;125(12):1216–24. <https://doi.org/10.1007/s11547-020-01215-w>.
 110. Granata V, Fusco R, Sansone M, Grassi R, Maio F, Palaia R, Tatangelo F, Botti G, Grimm R, Curley S, Avallone A, Izzo F, Petrillo A. Magnetic resonance imaging in the assessment of pancreatic cancer with quantitative parameter extraction by means of dynamic contrast-enhanced magnetic resonance imaging, diffusion kurtosis imaging and intravoxel incoherent motion diffusion-weighted imaging. *Therap Adv Gastroenterol.* 2020;13:1756284819885052. <https://doi.org/10.1177/1756284819885052>.
 111. Zhang A, Song J, Ma Z, Chen T. Combined dynamic contrast-enhanced magnetic resonance imaging and diffusion-weighted imaging to predict neoadjuvant chemotherapy effect in FIGO stage IB2-IIA2 cervical

- cancers. *Radiol Med.* 2020;125(12):1233–42. <https://doi.org/10.1007/s11547-020-01214-x>.
112. Sun NN, Ge XL, Liu XS, Xu LL. Histogram analysis of DCE-MRI for chemoradiotherapy response evaluation in locally advanced esophageal squamous cell carcinoma. *Radiol Med.* 2020;125(2):165–76. <https://doi.org/10.1007/s11547-019-01081-1>.
 113. Shannon BA, Ahlawat S, Morris CD, Levin AS, Fayad LM. Do contrast-enhanced and advanced MRI sequences improve diagnostic accuracy for indeterminate lipomatous tumors? *Radiol Med.* 2021. <https://doi.org/10.1007/s11547-021-01420-1>.
 114. Kawaguchi M, Kato H, Nagasawa T, Kaneko Y, Taguchi K, Ikeda T, Morita H, Miyazaki T, Matsuo M. MR imaging findings of musculoskeletal involvement in microscopic polyangiitis: a comparison with inflammatory myopathy. *Radiol Med.* 2021;126(12):1601–8. <https://doi.org/10.1007/s11547-021-01407-y>.
 115. Cellina M, Gibelli D, Martinenghi C, Giardini D, Soresina M, Menozzi A, Oliva G, Carrafiello G. Non-contrast magnetic resonance lymphography (NCML) in cancer-related secondary lymphedema: acquisition technique and imaging findings. *Radiol Med.* 2021;126(11):1477–86. <https://doi.org/10.1007/s11547-021-01410-3>.
 116. Maetani Y, Itoh K, Watanabe C, et al. MR imaging of intrahepatic cholangiocarcinoma with pathologic correlation. *AJR.* 2001;176:1499–507.
 117. Petralia G, Summers PE, Agostini A, Ambrosini R, Cianci R, Cristel G, Calistri L, Colagrande S. Dynamic contrast-enhanced MRI in oncology: how we do it. *Radiol Med.* 2020;125(12):1288–300. <https://doi.org/10.1007/s11547-020-01220-z>.
 118. Minutoli F, Pergolizzi S, Blandino A, Mormina E, Amato E, Gaeta M. Effect of granulocyte colony-stimulating factor on bone marrow: evaluation by intravoxel incoherent motion and dynamic contrast-enhanced magnetic resonance imaging. *Radiol Med.* 2020;125(3):280–7. <https://doi.org/10.1007/s11547-019-01115-8>.
 119. Fusco R, Sansone M, Granata V, Grimm R, Pace U, Delrio P, Tatangelo F, Botti G, Avallone A, Pecori B, Petrillo A. Diffusion and perfusion MR parameters to assess preoperative short-course radiotherapy response in locally advanced rectal cancer: a comparative exploratory study among Standardized Index of Shape by DCE-MRI, intravoxel incoherent motion- and diffusion kurtosis imaging-derived parameters. *Abdom Radiol (NY).* 2019;44(11):3683–700. <https://doi.org/10.1007/s00261-018-1801-z>.
 120. Lin CC, Cheng YF, Chiang HJ, et al. Pharmacokinetic analysis of dynamic contrast-enhanced magnetic resonance imaging for distinguishing hepatocellular carcinoma from cholangiocarcinoma in pre-liver transplantation evaluation. *Transplant Proc.* 2016;48:1041–4. <https://doi.org/10.1016/j.transproceed.2015.11.026>.
 121. Banerji A, Naish JH, Watson Y, et al. DCE-MRI model selection for investigating disruption of microvascular function in livers with metastatic disease. *J Magn Reson Imaging.* 2012;35:196–203.
 122. Khalifa F, Soliman A, El-Baz A, Abou El-Ghar M, El-Diasty T, Gimel'farb G, Ouseph R, Dwyer AC. Models and methods for analyzing DCE-MRI: a review. *Med Phys.* 2014;41:124301. <https://doi.org/10.1118/1.4898202>.
 123. Mungai F, Verrone GB, Bonasera L, Bicci E, Pietragalla M, Nardi C, Berti V, Mazzoni LN, Miele V. Imaging biomarkers in the diagnosis of salivary gland tumors: the value of lesion/parenchyma ratio of perfusion-MR pharmacokinetic parameters. *Radiol Med.* 2021;126(10):1345–55. <https://doi.org/10.1007/s11547-021-01376-2>.
 124. Russo L, Gui B, Miccò M, Panico C, De Vincenzo R, Fanfani F, Scambia G, Manfredi R. The role of MRI in cervical cancer > 2 cm (FIGO stage IB2-IIA1) conservatively treated with neoadjuvant chemotherapy followed by conization: a pilot study. *Radiol Med.* 2021;126(8):1055–63. <https://doi.org/10.1007/s11547-021-01377-1>.
 125. Jin KP, Sheng RF, Yang C, Zeng MS. Combined arterial and delayed enhancement patterns of MRI assist in prognostic prediction for intrahepatic mass-forming cholangiocarcinoma (IMCC). *Abdom Radiol (NY).* 2021. <https://doi.org/10.1007/s00261-021-03292-5>.
 126. Tan J, Sun X, Wang S, Ma B, Chen Z, Shi Y, Zhang L, Shah MA. Evaluation of angiogenesis and pathological classification of extrahepatic cholangiocarcinoma by dynamic MR imaging for E-healthcare. *J Healthc Eng.* 2021;2021:8666498. <https://doi.org/10.1155/2021/8666498>.
 127. Zhou Y, Zhou G, Zhang J, Xu C, Wang X, Xu P. Radiomics signature on dynamic contrast-enhanced MR images: a potential imaging biomarker for prediction of microvascular invasion in mass-forming intrahepatic cholangiocarcinoma. *Eur Radiol.* 2021;31(9):6846–55. <https://doi.org/10.1007/s00330-021-07793-1>.
 128. Lin CC, Cheng YF, Chiang HJ, Lazo M, Chang CD, Tsang LL, Yu CY, Hsu HW, Chen WT, Wang CC, Liang JL, Eng HL, Chen CL, Ou HY. Pharmacokinetic analysis of dynamic contrast-enhanced magnetic resonance imaging for distinguishing hepatocellular carcinoma from cholangiocarcinoma in pre-liver transplantation evaluation. *Transplant Proc.* 2016;48(4):1041–4. <https://doi.org/10.1016/j.transproceed.2015.11.026>.
 129. Konstantinidis IT, Do RK, Gultekin DH, Gönen M, Schwartz LH, Fong Y, Allen PJ, D'Angelica MI, DeMatteo RP, Klimstra DS, Kemeny NE, Jarnagin WR. Regional chemotherapy for unresectable intrahepatic cholangiocarcinoma: a potential role for dynamic magnetic resonance imaging as an imaging biomarker and a survival update from two prospective clinical trials. *Ann Surg Oncol.* 2014;21(8):2675–83. <https://doi.org/10.1245/s10434-014-3649-y>.
 130. Albano D, Stecco A, Micci G, Sconfienza LM, Colagrande S, Reginelli A, Grassi R, Carriero A, Midiri M, Lagalla R, Galia M. Whole-body magnetic resonance imaging (WB-MRI) in oncology: an Italian survey. *Radiol Med.* 2021;126(2):299–305. <https://doi.org/10.1007/s11547-020-01242-7>.
 131. Taverna C, Novelli L, De Renzis AGD, Calistri L, Tomei M, Occhipinti M, Colagrande S. The role of diffusion-weighted and dynamic contrast enhancement perfusion-weighted imaging in the evaluation of salivary glands neoplasms. *Radiol Med.* 2020;125(9):851–63. <https://doi.org/10.1007/s11547-020-01182-2>.
 132. Lian S, Zhang C, Chi J, Huang Y, Shi F, Xie C. Differentiation between nasopharyngeal carcinoma and lymphoma at the primary site using whole-tumor histogram analysis of apparent diffusion coefficient maps. *Radiol Med.* 2020;125(7):647–53. <https://doi.org/10.1007/s11547-020-01152-8>.
 133. Zhang Y, Zhu Y, Zhang K, Liu Y, Cui J, Tao J, Wang Y, Wang S. Invasive ductal breast cancer: preoperative predict Ki-67 index based on radiomics of ADC maps. *Radiol Med.* 2020;125(2):109–16. <https://doi.org/10.1007/s11547-019-01100-1>.
 134. Fornell-Perez R, Vivas-Escalona V, Aranda-Sanchez J, Gonzalez-Dominguez MC, Rubio-Garcia J, Aleman-Flores P, Lozano-Rodriguez A, Porcel-de-Peralta G, Loro-Ferrer JF. Primary and post-chemoradiotherapy MRI detection of extramural venous invasion in rectal cancer: the role of diffusion-weighted imaging. *Radiol Med.* 2020;125(6):522–30. <https://doi.org/10.1007/s11547-020-01137-7>.
 135. Koh DM, Collins DJ. Diffusion-weighted MRI in the body: applications and challenges in oncology. *AJR Am J Roentgenol.* 2007;188(6):1622–35. <https://doi.org/10.2214/AJR.06.1403>.
 136. Barnes A, Alonzi R, Blackledge M, Charles-Edwards G, Collins DJ, Cook G, Coultas G, Goh V, Graves M, Kelly C, Koh DM, McCallum H, Miquel ME, O'Connor J, Padhani A, Pearson R, Priest A, Rockall A, Stirling J, Taylor S, Tunariu N, van der Meulen J, Walls D, Winfield J, Punwani S. UK quantitative WB-DWI technical workgroup: consensus meeting recommendations on optimisation, quality control, processing and analysis of quantitative whole-body diffusion-weighted imaging for cancer. *Br J Radiol.* 2018;91(1081):20170577. <https://doi.org/10.1259/bjr.20170577>.
 137. Danti G, Flammia F, Matteuzzi B, Cozzi D, Berti V, Grazzini G, Pradella S, Recchia L, Brunese L, Miele V. Gastrointestinal neuroendocrine neoplasms (GI-NENs): hot topics in morphological, functional, and prognostic imaging. *Radiol Med.* 2021;126(12):1497–507. <https://doi.org/10.1007/s11547-021-01408-x>.
 138. Petralia G, Zugni F, Summers PE, Colombo A, Pricolo P, Grazioli L, Colagrande S, Giovagnoni A, Padhani AR; Italian Working Group on Magnetic Resonance. Whole-body magnetic resonance imaging (WB-MRI) for cancer screening: recommendations for use. *Radiol Med.* 2021;126(11):1434–1450. <https://doi.org/10.1007/s11547-021-01392-2>.
 139. Negroni D, Cassarà A, Trisoglio A, Soligo E, Berardo S, Carriero A, Stecco A. Learning curves in radiological reporting of whole-body MRI in plasma cell disease: a retrospective study. *Radiol Med.* 2021;126(11):1451–9. <https://doi.org/10.1007/s11547-021-01391-3>.
 140. Egnell L, Jerome NP, Andreassen MMS, Bathen TF, Goa PE. Effects of echo time on IVIM quantifications of locally advanced breast cancer in clinical diffusion-weighted MRI at 3 T. *NMR Biomed.* 2021. <https://doi.org/10.1002/nbm.4654>.
 141. Tavakoli AA, Dreher C, Mlynarska A, Kuder TA, Gnirs R, Schlemmer HP, Bickelhaupt S. Pancreatic imaging using diffusivity mapping—influence

- of sequence technique on qualitative and quantitative analysis. *Clin Imaging*. 2021;83:33–40. <https://doi.org/10.1016/j.clinimag.2021.11.033>.
142. Galati F, Trimboli RM, Pediconi F. Special Issue "Advances in Breast MRI". *Diagnostics (Basel)*. 2021;11(12):2297. <https://doi.org/10.3390/diagnostics11122297>
 143. Ogura A, Sotome H, Asai A, Fujii A. Evaluation of capillary blood volume in the lower limb muscles after exercise by intravoxel incoherent motion. *Radiol Med*. 2020;125(5):474–80. <https://doi.org/10.1007/s11547-020-01163-5>.
 144. Dyvorne H, Jajamovich G, Kakite S, Kuehn B, Taouli B. Intravoxel incoherent motion diffusion imaging of the liver: optimal b-value subsampling and impact on parameter precision and reproducibility. *Eur J Radiol*. 2014;83(12):2109–13. <https://doi.org/10.1016/j.ejrad.2014.09.003>.
 145. Granata V, Fusco R, Catalano O, Guarino B, Granata F, Tatangelo F, Avallone A, Piccirillo M, Palaia R, Izzo F, Petrillo A. Intravoxel incoherent motion (IVIM) in diffusion-weighted imaging (DWI) for Hepatocellular carcinoma: correlation with histologic grade. *Oncotarget*. 2016;7(48):79357–64. <https://doi.org/10.18632/oncotarget.12689>.
 146. Le Bihan D. What can we see with IVIM MRI? *Neuroimage*. 2019;187:56–67. <https://doi.org/10.1016/j.neuroimage.2017.12.062>.
 147. Iima M. Perfusion-driven intravoxel incoherent motion (IVIM) MRI in oncology: applications, challenges, and future trends. *Magn Reson Med Sci*. 2020. <https://doi.org/10.2463/mrms.rev.2019-0124>.
 148. Granata V, Fusco R, Catalano O, Filice S, Amato DM, Nasti G, Avallone A, Izzo F, Petrillo A. Early assessment of colorectal cancer patients with liver metastases treated with antiangiogenic drugs: the role of intravoxel incoherent motion in diffusion-weighted imaging. *PLoS ONE*. 2015;10(11):e0142876. <https://doi.org/10.1371/journal.pone.0142876>.
 149. Jensen JH, Helpert JA. MRI quantification of non-Gaussian water diffusion by kurtosis analysis. *NMR Biomed*. 2010;23(7):698–710. <https://doi.org/10.1002/nbm.1518>.
 150. Rosenkrantz AB, Padhani AR, Chenevert TL, Koh DM, De Keyzer F, Taouli B, Le Bihan D. Body diffusion kurtosis imaging: Basic principles, applications, and considerations for clinical practice. *J Magn Reson Imaging*. 2015;42(5):1190–202. <https://doi.org/10.1002/jmri.24985>.
 151. Granata V, Fusco R, Reginelli A, Delrio P, Selvaggi F, Grassi R, Izzo F, Petrillo A. Diffusion kurtosis imaging in patients with locally advanced rectal cancer: current status and future perspectives. *J Int Med Res*. 2019;47(6):2351–60. <https://doi.org/10.1177/0300060519827168>.
 152. Xu CC, Tang YF, Ruan XZ, Huang QL, Sun L, Li J. The value of Gd-BOPTA-enhanced MRIs and DWI in the diagnosis of intrahepatic mass-forming cholangiocarcinoma. *Neoplasma*. 2017;64(6):945–53. https://doi.org/10.4149/neo_2017_619.
 153. Kovač JD, Galun D, Đurić-Stefanović A, Lilić G, Vasin D, Lazić L, Mašulović D, Šaranović Đ. Intrahepatic mass-forming cholangiocarcinoma and solitary hypovascular liver metastases: is the differential diagnosis using diffusion-weighted MRI possible? *Acta Radiol*. 2017;58(12):1417–26. <https://doi.org/10.1177/0284185117695666>.
 154. Park HJ, Kim YK, Park MJ, Lee WJ. Small intrahepatic mass-forming cholangiocarcinoma: target sign on diffusion-weighted imaging for differentiation from hepatocellular carcinoma. *Abdom Imaging*. 2013;38(4):793–801. <https://doi.org/10.1007/s00261-012-9943-x>.
 155. Kovač JD, Daković M, Janković A, Mitrović M, Dugalić V, Galun D, Đurić-Stefanović A, Mašulović D. The role of quantitative diffusion-weighted imaging in characterization of hypovascular liver lesions: A prospective comparison of intravoxel incoherent motion derived parameters and apparent diffusion coefficient. *PLoS ONE*. 2021;16(2):e0247301. <https://doi.org/10.1371/journal.pone.0247301>.
 156. Zou X, Luo Y, Li Z, Hu Y, Li H, Tang H, Shen Y, Hu D, Kamel IR. Volumetric apparent diffusion coefficient histogram analysis in differentiating intrahepatic mass-forming cholangiocarcinoma from hepatocellular carcinoma. *J Magn Reson Imaging*. 2019;49(4):975–83. <https://doi.org/10.1002/jmri.26253>.
 157. Vernuccio F, Porrello G, Cannella R, Vernuccio L, Midiri M, Giannitrapani L, Soresi M, Brancatelli G. Benign and malignant mimickers of infiltrative hepatocellular carcinoma: tips and tricks for differential diagnosis on CT and MRI. *Clin Imaging*. 2021;70:33–45. <https://doi.org/10.1016/j.clinimag.2020.10.011>.
 158. Vernuccio F, Cannella R, Meyer M, Choudhury KR, Gonzáles F, Schwartz FR, Gupta RT, Bashir MR, Furlan A, Marin D. LI-RADS: diagnostic performance of hepatobiliary phase hypointensity and major imaging features of LR-3 and LR-4 lesions measuring 10–19 mm with arterial phase hyperenhancement. *AJR Am J Roentgenol*. 2019;213(2):W57–65. <https://doi.org/10.2214/AJR.18.20979>.
 159. Cannella R, Vernuccio F, Sagreya H, Choudhury KR, Iranpour N, Marin D, Furlan A. Liver Imaging Reporting and Data System (LI-RADS) v2018: diagnostic value of ancillary features favoring malignancy in hypervascular observations ≥ 10 mm at intermediate (LR-3) and high probability (LR-4) for hepatocellular carcinoma. *Eur Radiol*. 2020;30(7):3770–81. <https://doi.org/10.1007/s00330-020-06698-9>.
 160. Shao S, Shan Q, Zheng N, Wang B, Wang J. Role of intravoxel incoherent motion in discriminating hepatitis B virus-related intrahepatic mass-forming cholangiocarcinoma from hepatocellular carcinoma based on liver imaging reporting and data system v2018. *Cancer Biother Radiopharm*. 2019;34(8):511–8. <https://doi.org/10.1089/cbr.2019.2799>.
 161. Peng J, Zheng J, Yang C, Wang R, Zhou Y, Tao YY, Gong XQ, Wang WC, Zhang XM, Yang L. Intravoxel incoherent motion diffusion-weighted imaging to differentiate hepatocellular carcinoma from intrahepatic cholangiocarcinoma. *Sci Rep*. 2020;10(1):7717. <https://doi.org/10.1038/s41598-020-64804-9>.
 162. Fusco R, Granata V, Pariante P, Cerciello V, Siani C, Di Bonito M, Valentino M, Sansone M, Botti G, Petrillo A. Blood oxygenation level dependent magnetic resonance imaging and diffusion weighted MRI imaging for benign and malignant breast cancer discrimination. *Magn Reson Imaging*. 2021;75:51–9. <https://doi.org/10.1016/j.mri.2020.10.008>.
 163. Park HJ, Kim YK, Min JH, Lee WJ, Choi D, Rhim H. Feasibility of blood oxygenation level-dependent MRI at 3T in the characterization of hepatic tumors. *Abdom Imaging*. 2014;39(1):142–52. <https://doi.org/10.1007/s00261-013-0044-2>.
 164. Ria F, Samei E. Is regulatory compliance enough to ensure excellence in medicine? *Radiol Med*. 2020;125:904–5. <https://doi.org/10.1007/s11547-020-01171-5>.
 165. Crimi F, Capelli G, Spolverato G, Bao QR, Florio A, Milite Rossi S, Cecchin D, Albertoni L, Campi C, Pucciarelli S, et al. MRI T2-weighted sequences-based texture analysis (TA) as a predictor of response to neoadjuvant chemo-radiotherapy (nCRT) in patients with locally advanced rectal cancer (LARC). *Radiol Med*. 2020;125:1216–24. <https://doi.org/10.1007/s11547-020-01215-w>.
 166. Kirienco M, Ninatti G, Cozzi L, Voulaz E, Gennaro N, Barajon I, Ricci F, Carlo-Stella C, Zucali P, Sollini M, et al. Computed tomography (CT)-derived radiomic features differentiate prevascular mediastinum masses as thymic neoplasms versus lymphomas. *Radiol Med*. 2020;125:951–60. <https://doi.org/10.1007/s11547-020-01188-w>.
 167. Zhang L, Kang L, Li G, Zhang X, Ren J, Shi Z, Li J, Yu S. Computed tomography-based radiomics model for discriminating the risk stratification of gastrointestinal stromal tumors. *Radiol Med*. 2020;125:465–73. <https://doi.org/10.1007/s11547-020-01138-6>.
 168. Scapicchio C, Gabelloni M, Barucci A, Cioni D, Saba L, Neri E. A deep look into radiomics. *Radiol Med*. 2021;126(10):1296–311. <https://doi.org/10.1007/s11547-021-01389-x>.
 169. Wei J, Jiang H, Gu D, Niu M, Fu F, Han Y, Song B, Tian J. Radiomics in liver diseases: current progress and future opportunities. *Liver Int*. 2020;40(9):2050–63. <https://doi.org/10.1111/liv.14555>.
 170. Saini A, Breen I, Pershad Y, Naidu S, Knuttinen MG, Alzubaidi S, Sheth R, Albadawi H, Kuo M, Oklu R. Radiogenomics and radiomics in liver cancers. *Diagnostics (Basel)*. 2018;9(1):4. <https://doi.org/10.3390/diagnostics9010004>.
 171. Benedetti G, Mori M, Panzeri MM, Barbera M, Palumbo D, Sini C, Muffatti F, Andreasi V, Steidler S, Doglioni C, Partelli S, Manzoni M, Falconi M, Fiorino C, De Cobelli F. CT-derived radiomic features to discriminate histologic characteristics of pancreatic neuroendocrine tumors. *Radiol Med*. 2021. <https://doi.org/10.1007/s11547-021-01333-z>.
 172. Agazzi GM, Ravanelli M, Roca E, Medicina D, Balzarini P, Pessina C, Verri W, Berruti A, Maroldi R, Farina D. CT texture analysis for prediction of EGFR mutational status and ALK rearrangement in patients with non-small cell lung cancer. *Radiol Med*. 2021. <https://doi.org/10.1007/s11547-020-01323-7>.
 173. Santone A, Brunese MC, Donnarumma F, Guerriero P, Mercaldo F, Reginelli A, Miele V, Giovagnoni A, Brunese L. Radiomic features for prostate cancer grade detection through formal verification. *Radiol Med*. 2021;126(5):688–97. <https://doi.org/10.1007/s11547-020-01314-8>.

174. Cusumano D, Meijer G, Lenkovic J, Chiloiro G, Boldrini L, Masciocchi C, Dinapoli N, Gatta R, Casà C, Damiani A, Barbaro B, Gambacorta MA, Azario L, De Spirito M, Intven M, Valentini V. A field strength independent MR radiomics model to predict pathological complete response in locally advanced rectal cancer. *Radiol Med*. 2021;126(3):421–9. <https://doi.org/10.1007/s11547-020-01266-z>.
175. Hu HT, Shan QY, Chen SL, Li B, Feng ST, Xu EJ, Li X, Long JY, Xie XY, Lu MD, Kuang M, Shen JX, Wang W. CT-based radiomics for preoperative prediction of early recurrent hepatocellular carcinoma: technical reproducibility of acquisition and scanners. *Radiol Med*. 2020;125(8):697–705. <https://doi.org/10.1007/s11547-020-01174-2>.
176. Paoletti M, Muzic SJ, Marchetti F, Farina LM, Bastianello S, Pichiechio A. Differential imaging of atypical demyelinating lesions of the central nervous system. *Radiol Med*. 2021. <https://doi.org/10.1007/s11547-021-01334-y>.
177. Nazari M, Shirri I, Hajianfar G, Oveisi N, Abdollahi H, Deevband MR, Oveisi M, Zaidi H. Noninvasive Fuhrman grading of clear cell renal cell carcinoma using computed tomography radiomic features and machine learning. *Radiol Med*. 2020;125(8):754–62. <https://doi.org/10.1007/s11547-020-01169-z>.
178. Fusco R, Granata V, Mazzei MA, Meglio ND, Roscio DD, Moroni C, Monti R, Cappabianca C, Picone C, Neri E, Coppola F, Montanino A, Grassi R, Petrillo A, Miele V. Quantitative imaging decision support (QIDS™) tool consistency evaluation and radiomic analysis by means of 594 metrics in lung carcinoma on chest CT scan. *Cancer Control*. 2021;28:1073274820985786. <https://doi.org/10.1177/1073274820985786>.
179. Cellina M, Pirovano M, Ciocca M, Gibelli D, Floridi C, Oliva G. Radiomic analysis of the optic nerve at the first episode of acute optic neuritis: an indicator of optic nerve pathology and a predictor of visual recovery? *Radiol Med*. 2021;126(5):698–706. <https://doi.org/10.1007/s11547-020-01318-4>.
180. Qin H, Hu X, Zhang J, Dai H, He Y, Zhao Z, Yang J, Xu Z, Hu X, Chen Z. Machine-learning radiomics to predict early recurrence in perihilar cholangiocarcinoma after curative resection. *Liver Int*. 2021;41(4):837–50. <https://doi.org/10.1111/liv.14763>.
181. Hao X, Liu B, Hu X, Wei J, Han Y, Liu X, Chen Z, Li J, Bai J, Chen Y, Wang J, Niu M, Tian J. A Radiomics-based approach for predicting early recurrence in intrahepatic cholangiocarcinoma after surgical resection: a multicenter study. *Annu Int Conf IEEE Eng Med Biol Soc*. 2021;2021:3659–62. <https://doi.org/10.1109/EMBC46164.2021.9630029>.
182. Tang Y, Zhang T, Zhou X, Zhao Y, Xu H, Liu Y, Wang H, Chen Z, Ma X. The preoperative prognostic value of the radiomics nomogram based on CT combined with machine learning in patients with intrahepatic cholangiocarcinoma. *World J Surg Oncol*. 2021;19(1):45. <https://doi.org/10.1186/s12957-021-02162-0>.
183. Li MD, Lu XZ, Liu JF, Chen B, Xu M, Xie XY, Lu MD, Kuang M, Wang W, Shen SL, Chen LD. Preoperative survival prediction in intrahepatic cholangiocarcinoma using an ultrasound-based radiographic-radiomics signature. *J Ultrasound Med*. 2021. <https://doi.org/10.1002/jum.15833>.
184. Park HJ, Park B, Park SY, Choi SH, Rhee H, Park JH, Cho ES, Yeom SK, Park S, Park MS, Lee SS. Preoperative prediction of postsurgical outcomes in mass-forming intrahepatic cholangiocarcinoma based on clinical, radiologic, and radiomics features. *Eur Radiol*. 2021;31(11):8638–48. <https://doi.org/10.1007/s00330-021-07926-6>.
185. King MJ, Hectors S, Lee KM, Omidele O, Babb JS, Schwartz M, Tabrizian P, Taouli B, Lewis S. Outcomes assessment in intrahepatic cholangiocarcinoma using qualitative and quantitative imaging features. *Cancer Imaging*. 2020;20(1):43. <https://doi.org/10.1186/s40644-020-00323-0>.
186. Liang W, Xu L, Yang P, Zhang L, Wan D, Huang Q, Niu T, Chen F. Novel nomogram for preoperative prediction of early recurrence in intrahepatic cholangiocarcinoma. *Front Oncol*. 2018;8:360. <https://doi.org/10.3389/fonc.2018.00360>.
187. Ji GW, Zhu FP, Zhang YD, Liu XS, Wu FY, Wang K, Xia YX, Zhang YD, Jiang WJ, Li XC, Wang XH. A radiomics approach to predict lymph node metastasis and clinical outcome of intrahepatic cholangiocarcinoma. *Eur Radiol*. 2019;29(7):3725–35. <https://doi.org/10.1007/s00330-019-06142-7>.
188. Mosconi C, Cucchetti A, Bruno A, Cappelli A, Bargellini I, De Benedittis C, Lorenzoni G, Gramenzi A, Tarantino FP, Parini L, Pettinato V, Modestino F, Peta G, Cioni R, Golfieri R. Radiomics of cholangiocarcinoma on pretreatment CT can identify patients who would best respond to radioembolisation. *Eur Radiol*. 2020;30(8):4534–44. <https://doi.org/10.1007/s00330-020-06795-9>.
189. Xu H, Zou X, Zhao Y, Zhang T, Tang Y, Zheng A, Zhou X, Ma X. Differentiation of intrahepatic cholangiocarcinoma and hepatic lymphoma based on radiomics and machine learning in contrast-enhanced computer tomography. *Technol Cancer Res Treat*. 2021;20:15330338211039124. <https://doi.org/10.1177/15330338211039125>.
190. Peng YT, Zhou CY, Lin P, Wen DY, Wang XD, Zhong XZ, Pan DH, Que Q, Li X, Chen L, He Y, Yang H. Preoperative ultrasound radiomics signatures for noninvasive evaluation of biological characteristics of intrahepatic cholangiocarcinoma. *Acad Radiol*. 2020;27(6):785–97. <https://doi.org/10.1016/j.acra.2019.07.029>.
191. Deng L, Chen B, Zhan C, Yu H, Zheng J, Bao W, Deng T, Zheng C, Wu L, Yang Y, Yu Z, Wang Y, Chen G. A novel clinical-radiomics model based on sarcopenia and radiomics for predicting the prognosis of intrahepatic cholangiocarcinoma after radical hepatectomy. *Front Oncol*. 2021;11: 744311. <https://doi.org/10.3389/fonc.2021.744311>.
192. Li Q, Che F, Wei Y, Jiang HY, Zhang Y, Song B. Role of noninvasive imaging in the evaluation of intrahepatic cholangiocarcinoma: from diagnosis and prognosis to treatment response. *Expert Rev Gastroenterol Hepatol*. 2021;15(11):1267–79. <https://doi.org/10.1080/17474124.2021.1974294>.
193. Zhang J, Wu Z, Zhang X, Liu S, Zhao J, Yuan F, Shi Y, Song B. Machine learning: an approach to preoperatively predict PD-1/PD-L1 expression and outcome in intrahepatic cholangiocarcinoma using MRI biomarkers. *ESMO Open*. 2020;5(6):e000910. <https://doi.org/10.1136/esmoopen-2020-000910>.
194. Xue B, Wu S, Zheng M, Jiang H, Chen J, Jiang Z, Tian T, Tu Y, Zhao H, Shen X, Ramen K, Wu X, Zhang Q, Zeng Q, Zheng X. Development and validation of a radiomic-based model for prediction of intrahepatic cholangiocarcinoma in patients with intrahepatic lithiasis complicated by imagologically diagnosed mass. *Front Oncol*. 2021;10:598253. <https://doi.org/10.3389/fonc.2020.598253>.
195. Xu L, Wan Y, Luo C, Yang J, Yang P, Chen F, Wang J, Niu T. Integrating intratumoral and peritumoral features to predict tumor recurrence in intrahepatic cholangiocarcinoma. *Phys Med Biol*. 2021. <https://doi.org/10.1088/1361-6560/ac01f3>.
196. Wang Y, Shao J, Wang P, Chen L, Ying M, Chai S, Ruan S, Tian W, Cheng Y, Zhang H, Zhang X, Wang X, Ding Y, Liang W, Wu L. Deep learning radiomics to predict regional lymph node staging for hilar cholangiocarcinoma. *Front Oncol*. 2021;11:721460. <https://doi.org/10.3389/fonc.2021.721460>.
197. Tang Y, Yang CM, Su S, Wang WJ, Fan LP, Shu J. Machine learning-based Radiomics analysis for differentiation degree and lymphatic node metastasis of extrahepatic cholangiocarcinoma. *BMC Cancer*. 2021;21(1):1268. <https://doi.org/10.1186/s12885-021-08947-6>.
198. Zhao J, Zhang W, Zhu YY, Zheng HY, Xu L, Zhang J, Liu SY, Li FY, Song B. Development and validation of noninvasive mri-based signature for preoperative prediction of early recurrence in perihilar cholangiocarcinoma. *J Magn Reson Imaging*. 2021. <https://doi.org/10.1002/jmri.27846>.
199. Yao X, Huang X, Yang C, Hu A, Zhou G, Ju M, Lei J, Shu J. Correction: A novel approach to assessing differentiation degree and lymph node metastasis of extrahepatic cholangiocarcinoma: prediction using a radiomics-based particle swarm optimization and support vector machine model. *JMIR Med Inform*. 2021;9(1):e25337. <https://doi.org/10.2196/25337>. Erratum for: *JMIR Med Inform*. 2020;8(10):e23578.
200. Silva M, Maddalo M, Leoni E, Giuliotti S, Milanese G, Ghetti C, Biasini E, De Filippo M, Missale G, Sverzellati N. Integrated prognostication of intrahepatic cholangiocarcinoma by contrast-enhanced computed tomography: the adjunct yield of radiomics. *Abdom Radiol (NY)*. 2021;46(10):4689–700. <https://doi.org/10.1007/s00261-021-03183-9>.
201. Ren S, Li Q, Liu S, Qi Q, Duan S, Mao B, Li X, Wu Y, Zhang L. Clinical value of machine learning-based ultrasonomics in preoperative differentiation between hepatocellular carcinoma and intrahepatic cholangiocarcinoma: a multicenter study. *Front Oncol*. 2021;11:749137. <https://doi.org/10.3389/fonc.2021.749137>.
202. Xue B, Wu S, Zhang M, Hong J, Liu B, Xu N, Zeng Q, Tang K, Zheng X. A radiomic-based model of different contrast-enhanced CT phase for differentiate intrahepatic cholangiocarcinoma from inflammatory mass

- with hepatolithiasis. *Abdom Radiol (NY)*. 2021;46(8):3835–44. <https://doi.org/10.1007/s00261-021-03027-6>.
203. Zhao L, Ma X, Liang M, Li D, Ma P, Wang S, Wu Z, Zhao X. Prediction for early recurrence of intrahepatic mass-forming cholangiocarcinoma: quantitative magnetic resonance imaging combined with prognostic immunohistochemical markers. *Cancer Imaging*. 2019;19(1):49. <https://doi.org/10.1186/s40644-019-0234-4>.
 204. Aherne EA, Pak LM, Goldman DA, Gonen M, Jarnagin WR, Simpson AL, Do RK. Intrahepatic cholangiocarcinoma: can imaging phenotypes predict survival and tumor genetics? *Abdom Radiol (NY)*. 2018;43(10):2665–72. <https://doi.org/10.1007/s00261-018-1505-4>.
 205. Granata V, Fusco R, Risi C, Ottaiano A, Avallone A, De Stefano A, Grimm R, Grassi R, Brunese L, Izzo F, Petrillo A. Diffusion-weighted mri and diffusion kurtosis imaging to detect RAS mutation in colorectal liver metastasis. *Cancers (Basel)*. 2020;12(9):2420. <https://doi.org/10.3390/cancers12092420>.
 206. Granata V, Fusco R, Venanzio Setola S, Sandomenico F, Luisa Barretta M, Belli A, Palaia R, Tatangelo F, Grassi R, Izzo F, Petrillo A. Major and ancillary features according to LI-RADS in the assessment of combined hepatocellular-cholangiocarcinoma. *Radiol Oncol*. 2020;54(2):149–58. <https://doi.org/10.2478/raon-2020-0029>.
 207. Granata V, Fusco R, Setola SV, Picone C, Vallone P, Belli A, Incollingo P, Albino V, Tatangelo F, Izzo F, Petrillo A. Microvascular invasion and grading in hepatocellular carcinoma: correlation with major and ancillary features according to LI-RADS. *Abdom Radiol (NY)*. 2019;44(8):2788–800. <https://doi.org/10.1007/s00261-019-02056-6>.
 208. Fowler KJ, Potretzke TA, Hope TA, Costa EA, Wilson SR. LI-RADS M (LR-M): definite or probable malignancy, not specific for hepatocellular carcinoma. *Abdominal Radiol*. 2018;43(1):149–57. <https://doi.org/10.1007/s00261-017-1196-2>.
 209. Chernyak V, Fowler KJ, Kamaya A, Kielar AZ, Elsayes KM, Bashir MR, et al. Liver Imaging reporting and data system (LI-RADS) version 2018: imaging of hepatocellular carcinoma in at-risk patients. *Radiology*. 2018;289(3):816–30. <https://doi.org/10.1148/radiol.2018181494>.
 210. Kamath A, Roudenko A, Hecht E, Sirlin C, Chernyak V, Fowler K, et al. CT/MR LI-RADS 2018: clinical implications and management recommendations. *Abdominal Radiol*. 2019;44(4):1306–22. <https://doi.org/10.1007/s00261-018-1868-6>.
 211. Dietrich CF, Nolsoe CP, Barr RG, Berzigotti A, Burns PN, Cantisani V, et al. Guidelines and Good Clinical Practice Recommendations for Contrast-Enhanced Ultrasound (CEUS) in the liver-update 2020 WFUMB in cooperation with EFSUMB, AFSUMB, AIUM, and FLAUS. *Ultrasound Med Biol*. 2020;46(10):2579–604. <https://doi.org/10.1016/j.ultrasmedbio.2020.04.030>.
 212. Jo PC, Jang HJ, Burns PN, Burak KW, Kim TK, Wilson SR. Integration of contrast-enhanced US into a multimodality approach to imaging of nodules in a cirrhotic liver: how i do it. *Radiology*. 2017;282(2):317–31. <https://doi.org/10.1148/radiol.2016151732>.
 213. Kielar AZ, Chernyak V, Bashir MR, Do RK, Fowler KJ, Mitchell DG, et al. LI-RADS 2017: an update. *J magn reson Imaging JMRI*. 2018;47(6):1459–74. <https://doi.org/10.1002/jmri.26027>.
 214. An C, Lee CH, Byun JH, Lee MH, Jeong WK, Choi SH, et al. Intraindividual comparison between gadoxetate-enhanced magnetic resonance imaging and dynamic computed tomography for characterizing focal hepatic lesions: a multicentre, multireader study Korean. *J Radiol*. 2019;20(12):1616–26. <https://doi.org/10.3348/kjr.2019.0363>.
 215. Kim YY, Kim MJ, Kim EH, Roh YH, An C. Hepatocellular carcinoma versus other hepatic malignancy in cirrhosis: performance of LI-RADS version 2018. *Radiology*. 2019;291(1):72–80. <https://doi.org/10.1148/radiol.2019181995>.
 216. Zheng W, Li Q, Zou XB, Wang JW, Han F, Li F, et al. Evaluation of contrast-enhanced US LI-RADS version 2017: application on 2020 liver nodules in patients with hepatitis B infection. *Radiology*. 2020;294(2):299–307. <https://doi.org/10.1148/radiol.2019190878>.
 217. Marrero JA, Kulik LM, Sirlin CB, Zhu AX, Finn RS, Abecassis MM, et al. Diagnosis, staging, and management of hepatocellular carcinoma: 2018 practice guidance by the American association for the study of liver diseases. *Hepatology*. 2018;68(2):723–50. <https://doi.org/10.1002/hep.29913>.
 218. Zeng D, Xu M, Liang JY, Cheng MQ, Huang H, Pan JM, Huang Y, Tong WJ, Xie XY, Lu MD, Kuang M, Chen LD, Hu HT, Wang W. Using new criteria to improve the differentiation between HCC and non-HCC malignancies: clinical practice and discussion in CEUS LI-RADS 2017. *Radiol Med*. 2021. <https://doi.org/10.1007/s11547-021-01417-w>.
 219. Pignata S, Gallo C, Daniele B, Elba S, Giorgio A, Capuano G, Adinolfi LE, De Sio I, Izzo F, Farinati F, Del Naja C, Stanzione M, Castiglione F, Marone G, Cuomo O, Felder M, Gaeta GB, De Maio E, Di Maio M, Signoriello G, Perrone F; CLIP Investigators. Characteristics at presentation and outcome of hepatocellular carcinoma (HCC) in the elderly. A study of the Cancer of the Liver Italian Program (CLIP). *Crit Rev Oncol Hematol*. 2006;59(3):243–9.
 220. Perrone F, Gallo C, Daniele B, Gaeta GB, Izzo F, Capuano G, Adinolfi LE, Mazzanti R, Farinati F, Elba S, Piai G, Calandra M, Stanzione M, Mattered D, Aiello A, De Sio I, Castiglione F, Russo M, Persico M, Felder M, Manghisi OG, De Maio E, Di Maio M, Pignata S; Cancer of Liver Italian Program (CLIP) Investigators. Tamoxifen in the treatment of hepatocellular carcinoma: 5-year results of the CLIP-1 multicentre randomised controlled trial. *Curr Pharm Des*. 2002;8(11):1013–9.

Publisher's Note

Springer Nature remains neutral with regard to jurisdictional claims in published maps and institutional affiliations.

Ready to submit your research? Choose BMC and benefit from:

- fast, convenient online submission
- thorough peer review by experienced researchers in your field
- rapid publication on acceptance
- support for research data, including large and complex data types
- gold Open Access which fosters wider collaboration and increased citations
- maximum visibility for your research: over 100M website views per year

At BMC, research is always in progress.

Learn more biomedcentral.com/submissions

